GE: Erik Schelbert

The Future of Cardiac Magnetic Resonance Clinical Trials: A Society for Cardiovascular Magnetic Resonance White Paper

Brief Title: Future CMR Clinical Trials

Mark G. Rabbat, MD[a,b], Raymond Y. Kwong, MD, MPH[c], John F. Heitner, MD[d], Alistair A. Young, PhD[e], Sujata M. Shanbhag, MD[f], Steffen E. Petersen, MSc, MPH, MD, DPhil[g,h], Joseph B. Selvanayagam, MBBS (Hons) DPhil[i], Colin Berry, MD, PhD[j], Eike Nagel, MD[k], Bobak Heydari, MD, MPH[l], Alicia M. Maceira, MD[m], Chetan Shenoy, MD[n], Christopher Dyke, MD[o], Kenneth C. Bilchick, MD, MS[p]

[a] Division of Cardiology, Loyola University Chicago, Chicago, IL. USA. mrabbat@lumc.edu
[b] Division of Cardiology, Edward Hines Jr. VA Hospital, Hines, IL. USA. mrabbat@lumc.edu
[c] Cardiovascular Division, Department of Medicine, Brigham and Women's Hospital. rykwong@partners.org
[d] Department of Medicine, New York-Presbyterian Brooklyn Methodist Hospital, Brooklyn. USA. john.heitner@gmail.com
[e] Department of Biomedical Engineering, King's College London, London, UK. alistair.young@kcl.ac.uk
[f] National Heart, Lung, and Blood Institute, National Institutes of Health, Bethesda, Maryland. USA. shanbhagsm@nhlbi.nih.gov
[g] Barts Heart Centre, St Bartholomew's Hospital, Barts Health NHS Trust, West Smithfield, London, UK. s.e.petersen@qmul.ac.uk
[h] NIHR Barts Biomedical Research Centre, William Harvey Research Institute, Queen Mary University of London, London, UK. s.e.petersen@qmul.ac.uk
[i] College of Medicine, Flinders University of South Australia; Department of Cardiovascular Medicine, Flinders Medical Centre, Southern Adelaide Local Health Network; Cardiac Imaging Research Group, South Australian Health and Medical Research Institute, Adelaide, South Australia. joseph.selvanayagam@flinders.edu.au
[j] West of Scotland Heart and Lung Centre, Golden Jubilee National Hospital, Glasgow, Scotland, UK; British Heart Foundation Glasgow Cardiovascular Research Centre, Institute of Cardiovascular and Medical Sciences, University of Glasgow, Scotland, UK. colin.berry@glasgow.ac.uk
[k] Institute for Experimental and Translational Cardiovascular Imaging, Klinikum der Johann Wolfgang Goethe-Universitat Frankfurt, Frankfurt am Main, Germany. eike.nagel@cardiac-imaging.org
[l] From the Stephenson Cardiac Imaging Centre and Department of Cardiac Sciences, Libin Cardiovascular Institute of Alberta, University of Calgary, Canada; Department of Cardiac Sciences, University of Calgary, Alberta, Canada. bobby.heydari@ucalgary.ca
[m] Cardiovascular Unit, Ascires Biomedical Group, Valencia, Spain. Department of Medicine, Health Sciences School, UCH-CEU University, Valencia, Spain. amaceira@ascires.com
[n] Cardiovascular Division, Department of Medicine, University of Minnesota Medical School, Minneapolis, USA. cshenoy@umn.edu
[o] Division of Cardiology, National Jewish Health, Denver, CO, USA. dykec@njhealth.org
[p] Division of Cardiovascular Medicine, University of Virginia Health System, Charlottesville, VA. USA. bilchick@virginia.edu

Total Word Count: 5,817 (including text, references, and figure legends)

Relationships with Industry: Dr. Petersen provides consultant services to and is a shareholder in Circle Cardiovascular Imaging, Inc. Dr. Nagel receives speaker fees, consulting fees, and grant support from Bayer AG and research grant support from NeoSoft. Dr. Bilchick has research grant support from Siemens Healthineers and Medtronic, Inc.

Funding: There was no funding received for the work presented in this manuscript.

Corresponding Author:
Raymond Y. Kwong, MD MPH
Director of Cardiac Magnetic Resonance Imaging
Cardiovascular Division, Department of Medicine, Brigham and Women's Hospital
Professor of Medicine, Harvard Medical School
75 Francis Street,
Boston, MA 02115
Office: (617)-732-1960

Abstract

Over the past two decades, cardiac magnetic resonance imaging (CMR) has become an essential component of cardiovascular clinical care and contributed to imaging-guided diagnosis and management of coronary artery disease, cardiomyopathy, congenital heart disease, cardio-oncology, valvular and vascular disease, amongst others. The widespread availability, safety, and capability of CMR to provide corresponding anatomic, physiologic and functional data in one imaging session can improve the design and conduct of clinical trials both through reduction of sample size, and provision of important mechanistic data that may augment clinical trial findings. Moreover, prospective imaging-guided strategies using CMR can enhance safety, efficacy, and cost effectiveness of cardiovascular pathways in clinical practice around the world. As the future of large-scale clinical trial design evolves to integrate personalized medicine, cost-effectiveness, and mechanistic insights of novel therapies, the integration of CMR will continue to play a critical role. In this document, the attributes, limitations, and challenges of CMR's integration into the future design and conduct of clinical trials will also be covered and recommendations for trialists will be explored. Several prominent examples of clinical trials that test the efficacy of CMR-imaging guided pathways will also be discussed.

Keywords: clinical trials, cardiac magnetic resonance imaging

Abbreviations:
AI: Artificial Intelligence
ANOCA: angina and nonobstructive coronary artery disease
ARVC: Arrhythmogenic right ventricular cardiomyopathy
COVID-19: coronavirus disease 2019
CMR: cardiac magnetic resonance imaging
DENSE: displacement encoding with stimulated echoes
LGE: late gadolinium enhancement
NSTEMI/STEMI: (non-) ST elevation myocardial infarction
SCMR: Society for Cardiovascular Magnetic Resonance

CMR to Address Critical Needs in Healthcare

Cardiovascular disease remains the leading cause of morbidity and mortality worldwide. Accurate diagnosis is imperative to guide appropriate clinical decision-making that ultimately translates into improved patient outcomes. Cardiac magnetic resonance (1), a non-invasive imaging modality with excellent diagnostic and prognostic performance, has become the reference standard for numerous cardiovascular measurements. Advancements in CMR image acquisition and post-processing with the advent of parametric mapping provides a unique "virtual heart biopsy" for the clinician, with detailed myocardial structure, function, perfusion, and tissue characterization supporting its utility in the era of precision medicine. CMR may be conducted with or without gadolinium contrast, is highly conducive to serial imaging, and does not expose patients to ionizing radiation or iodinated contrast. These aggregate attributes make CMR imaging biomarkers particularly well suited as surrogate clinical trial endpoints for the evaluation of both novel pharmacologic and invasive interventions (2,3). In addition, technical CMR innovations have led to scanners becoming faster (with compression techniques), less expensive, more automated, and easier to use providing further benefits in the evaluation of cardiovascular disease.

CMR for Stable Coronary Disease Trials

There is extensive clinical evidence that stress CMR accurately diagnose patients with hemodynamically significant coronary stenosis, and in symptomatic patients, effectively guides the use of invasive coronary angiography and coronary revascularization (Figure 1). The MR-INFORM randomized control trial demonstrated that patients with stable angina at intermediate-high risk for coronary artery disease (CAD) showed non-inferior adverse outcomes at 1-year despite lower utilization of invasive therapies when guided by stress perfusion CMR first compared to an invasive fractional flow reserve (4) strategy

(Supplementary Table) (2). CE-MARC 2 was a multicenter, 3-parallel group, randomized clinical trial involving 1,202 patients with suspected CAD comparing stress perfusion CMR with nuclear perfusion imaging (MPI) and first-line cardiac computed tomography angiography (CTA) as per National Institute for Health and Care Excellence (NICE) guideline (3). CMR resulted in a lower probability of unnecessary invasive coronary angiography within 12 months than NICE guideline–directed care, with no statistically significant difference between CMR and MPI. CMR metrics in the MR-INFORM, (2) Stress CMR Perfusion Imaging in the United States (SPINS) (5) and EURO-CMR registries (6) have consistently demonstrated the ability of CMR to reduce unnecessary downstream procedures, minimize costs, while acting as a powerful risk stratification tool for identifying individuals at increased risk for adverse cardiac events. CMR may be particularly advantageous in future trials of CAD in women owing to its high specificity, prognostic utility, ability to characterize microvascular ischemia, and absence of thoracic radiation.

CMR for Acute Myocardial Infarction Trials

Echocardiography offers a rapid assessment of ventricular and valvular structure and function and it will continue to serve as a first-line tool after an acute myocardial infarction (AMI). However, CMR is uniquely suited to address the spectrum of myocardial tissue characteristics as a result of the acute injury (Figure 2) (7). CMR provides assessment of necrosis (irreversible damage) and surrounding edema (salvage area, reversible damage) in AMI, in addition to scaling the severity of ischemic injury using novel quantitative tissue mapping techniques (8). CMR has high diagnostic and prognostic values in recent AMI clinical trials, (9) (10) and served as surrogate endpoints of various novel therapeutic interventions. Infarct size by CMR has demonstrated incremental prognostic performance in STEMI patients beyond left ventricular systolic function (11). Microvascular obstruction

(MVO) and myocardial salvage index have shown incremental association with both LV functional recovery and future adverse cardiac events (12). Additional CMR paramaters, such as LV strain (13) and native T1-mapping have also shown incremental prognostic utility and the capability to differentiate between reversible and irreversible myocardial damage in acute STEMI (13). CMR may also play an important role in the diagnostic evaluation of challenging CAD sub-populations, such as women suffering AMI with non-obstructive coronary artery disease (MINOCA) as shown in the Heart Attack Research Program (HARP) (14). Multiparametric mapping and quantitative measures of myocardial blood flow by CMR are currently undergoing validation with invasive coronary vascular function reference standard for INOCA in the CORCMR substudy of the CORMICA trial (Supplementary Table) (15).

CMR for Valvular Heart Disease

Echocardiography provides efficient first-line assessment of severity of valular heart disease (VHD) and anatomical structures of the heart valves. However, CMR complements by providing a multifacet interrogation of valvular anatomy, quantitation of peak blood flow velocity across valves and regurgitant volumes/fractions, the consequential effects of VHD on ventricular dimensions and geometry, myocardial fibrosis (16), and reversal of left ventricular (LV) remodeling after valvular intervention. Multicenter trials have evaluated the prognostic value of CMR-derived parameters in aortic and mitral regurgitation (AR, MR) and aortic stenosis (AS) with the aim to find thresholds to guide valve surgery (Supplementary Table) (Figure 3) (17). CMR is especially useful when discordant information exists or poor-quality echocardiographic windows that compromise evaluation of valve lesion severity or ventricular volumes/function. A recent multicenter study (18) conducted in asymptomatic patients with moderate to severe MR reported that CMR-derived regurgitant volume and fraction of ≥55ml

and >40%, respectively, accurately identified patients with adverse prognosis that required surgery on follow-up. Quantification of AR severity by echocardiography may be challenging and CMR plays an important complementary role. Kammerlander et al demonstrated that quantitation of AR by CMR reclassified patients over echocardiography and provided incremental prognostic value that better guided time to aortic valve surgery (19). Another multicenter prospective study (18) of patients with moderate or severe AR observed that a CMR-derived regurgitant fraction of >33% in combination with a large LVEDV was associated with a rapid worsening clinical course towards needing valve surgery. Late gadolinium enhancement had been shown to provide incremental prognostic information complementary to morphological/functional parameters (20).

CMR methods may offer new direction in designing clinical trials of patients with aortic stenosis (AS). Echocardiography offers highly accurate quantitation of the severity of AS but both myocardial scar (21) and extracellular volume fraction (22) by CMR have demonstrated strong prognostic association with mortality in patients with severe aortic stenosis, thus potentially playing a role for planning of aortic valve replacement. Stress CMR-derived myocardial perfusion reserve, as a way characterizing coronary microvascular dysfunction, had also been shown to have specific prognostic values in patients with AS (23). The ongoing EVOLVED randomized trial is using CMR-derived LGE imaging to screen for mid-wall fibrosis in asymptomatic AS patients and is evaluating the benefits of early surgery compared to watchful waiting (24).

CMR for Chemotherapy Toxicity

Echocardiography has been the mainstay for the surveillance and detection of cardiovascular toxicity of chemotherapy, but CMR offers important information in the early identification

of structural and pathologic changes in cancer patients at risk and can inform therapeutic decision making. Compared to echocardiography, higher precision and accuracy by CMR to detect small, early changes in chamber size, ventricular function, native T1 values and global strain can inform therapeutic decisions. In addition, CMR is beneficial in scenarios with poor echocardiographic windows, conflicting results, or concern for ionization radiation. Tissue characterization techniques with LGE, ECV, T1, and T2 mapping assist in elucidating mechanisms of myocardial injury, such as edema, inflammation, interstitial or replacement fibrosis. The versatility of CMR as a single modality allows a comprehensive evaluation for a large spectrum of cardiovascular toxicities, including concomitant pericardial disease, underlying non-ischemic or ischemic etiologies for cardiac dysfunction (i.e. high diagnostic accuracy of stress CMR for coronary artery disease and microvascular dysfunction), and vascular toxicity (i.e. aortic distensibility) (25).

CMR for Cardiomyopathies

Amongst nonischemic cardiomyopathies, CMR tissue characterization techniques, such as LGE, T1/T2 mapping, ECV and T2* assessment have been established in diagnosis, risk stratification, and guidance of management (26) (Figure 4). Since ECV predicts survival and correlates with the severity of amyloidosis infiltration, it could be used as a surrogate endpoint in clinical trials of cardiac amyloidosis therapies. Since T1 is decreased before LGE is apparent in Anderson-Fabry disease, this could be used in clinical trials of early treatment with enzyme replacement (27). Tissue characterization could also be used in clinical trials testing the type and the duration of immunosuppression in inflammatory cardiomyopathies, such as cardiac sarcoidosis and giant cell myocarditis (Supplementary Table). CMR may also be useful in heart failure with preserved ejection fraction risk stratification, guiding treatment, and assessing treatment response (28). Overall, the role of CMR in addition to

echocardiography and other alternatives for nonischemic cardiomyopathy is widely recognized; however, additional clinical trials are needed to address evolving clinical management strategies.

CMR for Arrhythmia Risk Stratification in Heart Failure

While assessment of LV function and viability with other imaging modalities such as echocardiography, MPI, and CT can be useful for ventricular arrhythmia risk stratification in heart failure (29), the importance of CMR for this application is widely recognized. For example, CMR can identify key structural findings in both ischemic cardiomyopathy and non-ischemic cardiomyopathy, (30,31) including sarcoidosis (32), to identify the best candidates for implantable cardioverter defibrillators (Supplementary Table) (33). While echocardiography has also been studied for cardiac resynchronization therapy (34), CMR is particularly well-suited to identifying the best pacing strategies in patients with heart failure undergoing cardiac resynchronization therapy (35). In addition, CMR has been shown to be useful for identifying optimal targets for catheter ablation procedures in both ventricular tachycardia (36) and atrial fibrillation (37). In hypertrophic cardiomyopathy (HCM), LGE has been advocated for implantable cardioverter defibrillator risk stratification (38), and the ongoing Hypertrophic Cardiomyopathy Registry promises to further define the role of CMR in HCM (Supplementary Table) (39). In arrhythmogenic right ventricular cardiomyopathy (ARVC), abnormal CMR findings related to global and regional right ventricular function are advocated for diagnosis of ARVC (40) in combination with other criteria, and CMR findings including LGE are used for implantable cardioverter defibrillator risk stratification (Supplementary Table) (41). In cardiac sarcoidosis, current guidelines include LGE as a criterion to justify implantable cardioverter implantation (41). In patients with nonischemic cardiomyopathy, CMR can identify patients at increased risk for sudden cardiac death but not

included in current guidelines for primary prevention implantable cardioverter defibrillators (41), such as those with midwall LGE and left ventricular ejection fraction ≥40% (42,43). In addition, CMR is also used to assess for infiltrative disease in patients with nonischemic cardiomyopathy.

CMR for Ablation of Ventricular Tachycardia

CMR can produce models of regional electrical conduction velocities to identify the critical isthmus for ventricular tachycardia ablations (44). In specialized centers, LGE can be used to create maps that simulate voltage maps generated with invasive electroanatomic method (45). In patients with atrial fibrillation, left atrial fibrosis can be detected and quantified with LGE-CMR, although access to proprietory post-processing software remains limited. CMR characterized left atrial fibrosis prior to a first ablation can predict outcomes, and patients with more left atrial fibrosis may benefit from more extensive ablation in addition to the standard pulmonary vein isolation approach used in most patients (37,46). If quality of left atrial imaging improves, gaps in ablation lines after a catheter ablation procedure could be assessed in order to inform prognosis and design ablation strategies prior to a second ablation procedure.

CMR for Cardiac Manifestations of Coronavirus Infections

CMR may also be very useful for patients who have recovered from a coronavirus infection, particularly COVID-19. A recent CMR study with 100 patients demonstrated cardiac involvement in 78% and ongoing inflammation in 60% of recovered COVID-19 patients (47). The effects of COVID-19 on myocardial perfusion are being prospectively evaluated in the CISCO-19 multicenter study in the United Kingdom (48). CMR may play an important role in cardiac prognostication amongst patients with active and recovered COVID-19.

Infrastructure and Support for CMR Clinical Trials

The Society for Cardiovascular Magnetic Resonance (1) is actively providing resources and guidance to facilitate clinical trials in CMR. The SCMR standardized imaging protocols 2020 update describes current recommendations for field strength, appropriate pulse sequences, stress/contrast agents, device compatibility and acquisition protocols for common endpoints. General protocols for ventricular function, perfusion, LGE, flow quantification, and myocardial mapping (T1, T2 and T2*) are provided that should be followed by all sites in multi-center trials. Disease specific protocols are also included (Supplementary Table) (49). A companion statement outlines recommendations for post-processing and analysis (50). SCMR members can also search a list of members whose facilities conduct research studies (https://scmr.org/page/ResCtrDirPage). In addition, SCMR Clinical Trials Taskforce is working to support collaborative clinical trial efforts and recently summarized the evidence supporting the use of CMR endpoints in clinical trials (1).

The establishment of CMR registries has the potential to facilitate multi-center clinical trials. The European CMR Registry has demonstrated the impact of CMR on diagnosis and management (6) The SCMR Registry seeks to foster multi-center research and gather evidence for the impact of CMR on outcomes (42). Investigator-led CMR trials are beginning to be co-funded by industry, leveraging resources from the SCMR registry. For example, with funding support from industry, the SPINS trial (5) evaluated the prognostic value of stress CMR on 2,349 patients with stable angina and 2 or more risk factors followed for a median of 5.4 years, showing that patients with ischemia and positive LGE had >4-fold higher annual event rate within the first year. In contrast, those with no ischemia or LGE had a negative event rate of 99% over 5 years. The Hypertrophic Cardiomyopathy Registry,

facilitated by SCMR investigators, prospectively includes 2755 patients and intends to improve risk prediction in this population and to discover new genotype-phenotype relationships of patient sub-groups (39,51). The production of multi-center registries may be particularly important in congenital heart disease, in which data sharing is crucial to enable sufficient numbers for computational meta-analyses (52).

Components in Planning of a Clinical Trial Using CMR

The general approach to planning a clinical trial using CMR should include evaluation of the type of clinical study needed to address the clinical question of interest. CMR can be used to identify appropriate patients for testing an intervention, confirm similar distributions of key characteristics in treatment arms, develop appropriate surrogate endpoints, and inform the development of very large studies with hard clinical endpoints based on surrogate endpoints evaluated in previous CMR studies. The specific components of planning a clinical trial using CMR include:

1) Specification of the imaging-guided intervention and comparator;

2) Determination of the appropriate patient group for evaluation of these interventional strategies, and identification of primary and secondary endpoints;

3) Power analysis to identify the number of participants needed to answer the clinical question;

4) Consideration of whether a single-site or multi-site clinical trial is most appropriate regarding ability to achieve target enrollment and endpoint assessment;

5) A realistic balance between technical novelty of complex pulse sequence methods and feasibility and consistency of multicenter data acquisition;

6) Development of an *a priori* plan for statistical analysis of the study findings;

7) Specification of a Data Coordinating Center and Clinical Coordinating Center, governed by separate teams of leadership; and

8) Identification of the target funding source.

Standardization of All Imaging Reporting and Interpretation in a Clinical Trial

Standardization of CMR imaging reporting and interpretation is mandatory. For example, although CMR has been used in Phase 2a and 2b STEMI clinical trials for the assessment of infarct size and myocardial salvage (53,54), there is a need for international standardization of CMR parameters used to characterize edema, inflammation, microvascular obstruction, and other physiologic findings. Site training and initiation, imaging manuals, assessment of test cases and continuous quality control by a core laboratory all help to improve precision, standardization, and consequently the power of the trial.

Primary and Secondary Endpoints in CMR Clinical Trials

The value of various techniques as imaging biomarkers has been described in full detail in a consensus document, as shown in the summary in Table 1 (1). When using CMR as an endpoint in larger clinical trials, it may be advisable to use biomarkers with better validation as primary endpoints. As imaging biomarkers are usually surrogate endpoints in clinical trials, they ideally would be validated for a predictive association with hard endpoints, such as death or heart failure.

Health quality or quality of life are well established patient reported outcome measures that are routinely used in clinical trials and are essential components of health economic evaluations since costs are frequently measured in costs per quality life years gained. Training of sites in data acquisition methods is essential. A reasonable starting point for

endpoint standardization is the Societal Consensus Statements on data acquisition, postprocessing, reporting, analytical validation and clinical qualification, which provide a consensus among experts.

Limitations of CMR for Clinical Trial Endpoints and Cost Effectiveness

While the rapid evolution of CMR has provided a wealth of imaging biomarkers, assessment of multiple biomarkers in a single session can incrementally increase scan duration (55). Another consideration is that while surrogate imaging biomarkers may be highly sensitive for detection of particular cardiovascular disease processes, some imaging biomarkers may lack adequate specificity to serve as substitute trial endpoints. In accordance, many newer CMR sequences require adequate cardiac gating, heart rates, and breath-holding, such that site training and specification of protocols are necessary to obtain high-quality, consistent data in large, heterogeneous patient populations enrolled across multiple centers. Despite having similar sequences across CMR vendors, these sequences may have different normative values, particularly at different field strength. For this reason, standardization of CMR biomarkers prior to site inclusion/enrollment are critical (56). In the future, these challenges should be addressed on an international societal level to ensure the integrity and future evolution of CMR core laboratories to achieve reproducible and comparable CMR-imaging data for potential enrolling sites around the world.

CMR is not ideally suited for certain patient populations, such as pregnancy, non-compatible metallic devices, and known hypersensitivity to gadolinium. Recent data has shown exceedingly rare incidence of nephrogenic systemic fibrosis with administration of group II gadolinium contrast agents (57) leading to liberalization of MRI guidelines in patients with chronic kidney disease. In addition, novel sequences such as wideband LGE have

significantly improved image quality and can accurately localize myocardial scar in many patients with implantable electronic devices (58).

The current cost of CMR infrastructure serves as a potential limitation in clinical trials, particularly if less expensive imaging modalities may provide similar surrogate endpoint measures with non-inferior reproducibility. Fortunately, with the expanding clinical need for CMR, these issues will become less of a barrier in future as the capacity to conduct CMR improves worldwide along with commensurate decreases in costs. Moreover, mounting evidence for the superior cost-effectiveness of CMR over existing standard of care will further improve clinical adoption and cost-savings for healthcare systems (59,60).

Role of Artificial Intelligence and Machine Learning in CMR Clinical Trials

Artificial intelligence (AI) has the unique ability to aid patient selection, acquisition of images, post-processing of data and interpretation of sequences. AI can analyze both patient records and trial inclusion/exclusion criteria enabling physicians to quickly review a list of potential trials for patients, while supporting the clinical trial office in reaching enrollment numbers. Novel AI-guided MRI platforms prescribe the standard cardiac views, acquiring images more quickly, improves patient experience through fewer breath holds and reduces imaging artifacts from arrhythmia by using real-time imaging (61).

AI and machine learning can unravel the wealth of information contained in CMR images and potentially enhances patient diagnosis, prognosis and outcome predictions. Machine learning for automatic ventricular segmentation has been used to measure cardiac mass and function with high accuracy and reproducibility (62). Using deep neural networks, an automated method achieved a performance on par with human experts in analyzing CMR

images and deriving clinically relevant measures (63). Deep convolutional neural networks have been applied to automatically quantify LV mass and scar volume on LGE in patients with hypertrophic cardiomyopathy, with strong correlation between the automatic and manual segmentations (64).

AI is a promising approach for future clinical trials, but there are important potential ethical and legal ramifications. First, the incorporation of big data raises questions of privacy and security. Furthermore, risk for biases towards financial gain or worsening health disparities exist (65). Third, issues related to the "black box" algorithm and what happens when the human and algorithm disagree also need to be considered.

Conclusions

CMR is suited well to provide complementary information relative to other imaging modalities in order to help meet critical needs related to diagnosis and treatment of cardiovascular disease. In addition, CMR is well positioned to play an integral part in clinical trials with its ability to provide anatomic, physiologic and functional data in a single imaging session. In the era of personalized medicine, value-based care and mechanistic insights of novel therapies, the integration of CMR in clinical trials will continue to evolve.

References

1. Puntmann VO, Valbuena S, Hinojar R et al. Society for Cardiovascular Magnetic Resonance (SCMR) expert consensus for CMR imaging endpoints in clinical research: part I - analytical validation and clinical qualification. Journal of Cardiovascular Magnetic Resonance 2018;20:67-67.
2. Nagel E, Greenwood JP, McCann GP et al. Magnetic Resonance Perfusion or Fractional Flow Reserve in Coronary Disease. N Engl J Med 2019;380:2418-2428.
3. Greenwood JP, Ripley DP, Berry C et al. Effect of Care Guided by Cardiovascular Magnetic Resonance, Myocardial Perfusion Scintigraphy, or NICE Guidelines on Subsequent Unnecessary Angiography Rates: The CE-MARC 2 Randomized Clinical Trial. JAMA 2016;316:1051-60.
4. Maron DJ, Hochman JS, Reynolds HR et al. Initial Invasive or Conservative Strategy for Stable Coronary Disease. N Engl J Med 2020;382:1395-1407.
5. Kwong RY, Ge Y, Steel K, Al E. Cardiac Magnetic Resonance Stress Perfusion Imaging for Evaluation of Patients With Chest Pain. J Am Coll Cardiol 2019;74:1741-1755.
6. Bruder O, Wagner A, Lombardi M et al. European cardiovascular magnetic resonance (EuroCMR) registry – multi national results from 57 centers in 15 countries. Journal of Cardiovascular Magnetic Resonance 2013;15:9-9.
7. Friedrich MG, Abdel-Aty H, Taylor A, Schulz-Menger J, Messroghli D, Dietz R. The salvaged area at risk in reperfused acute myocardial infarction as visualized by cardiovascular magnetic resonance. J Am Coll Cardiol 2008;51:1581-7.
8. Messroghli DR, Moon JC, Ferreira VM et al. Clinical recommendations for cardiovascular magnetic resonance mapping of T1, T2, T2* and extracellular volume: A consensus statement by the Society for Cardiovascular Magnetic Resonance

(SCMR) endorsed by the European Association for Cardiovascular Imaging (EACVI). J Cardiovasc Magn Reson 2017;19:75.

9. Heitner JF, Senthilkumar A, Harrison JK et al. Identifying the Infarct-Related Artery in Patients With Non-ST-Segment-Elevation Myocardial Infarction. Circ Cardiovasc Interv 2019;12:e007305.

10. Hamo CE, Klem I, Rao SV et al. The Systematic Evaluation of Identifying the Infarct Related Artery Utilizing Cardiac Magnetic Resonance in Patients Presenting with ST-Elevation Myocardial Infarction. PLoS One 2017;12:e0169108.

11. Larose E, Rodes-Cabau J, Pibarot P et al. Predicting late myocardial recovery and outcomes in the early hours of ST-segment elevation myocardial infarction traditional measures compared with microvascular obstruction, salvaged myocardium, and necrosis characteristics by cardiovascular magnetic resonance. J Am Coll Cardiol 2010;55:2459-69.

12. Eitel I, Desch S, Fuernau G et al. Prognostic significance and determinants of myocardial salvage assessed by cardiovascular magnetic resonance in acute reperfused myocardial infarction. J Am Coll Cardiol 2010;55:2470-9.

13. Mangion K, Carrick D, Carberry J et al. Circumferential strain predicts major adverse cardiovascular events following an acute ST-segment-elevation myocardial infarction. Radiology 2018:181253.

14. Reynolds HR, Maehara A, Kwong RY et al. Coronary Optical Coherence Tomography and Cardiac Magnetic Resonance Imaging to Determine Underlying Causes of Myocardial Infarction With Nonobstructive Coronary Arteries in Women. Circulation 2021;143:624-640.

15. Corcoran D, Ford TJ, Hsu LY, et al. Rationale and design of the Coronary Microvascular Angina Cardiac Magnetic Resonance Imaging (CorCMR) diagnostic study: the CorMicA CMR sub-study. Open Heart 2018;5:e000924-e000924.
16. Sondergaard L, Thomsen C, Stahlberg F et al. Mitral and aortic valvular flow: quantification witn MR phase mapping. J Magn Reson Imaging 1992;2:295-302.
17. Hundley WG, Li HF, Willard JE et al. Magnetic resonance imaging assessment of the severity of mitral regurgitation. Comparison with invasive techniques. Circulation 1995;92:1151-8.
18. Myerson SG, d'Arcy J, Christiansen JP et al. Determination of Clinical Outcome in Mitral Regurgitation With Cardiovascular Magnetic Resonance Quantification. Circulation 2016;133:2287-96.
19. Kammerlander AA, Wiesinger M, Duca F et al. Diagnostic and Prognostic Utility of Cardiac Magnetic Resonance Imaging in Aortic Regurgitation. JACC Cardiovasc Imaging 2019;12:1474-1483.
20. Malahfji M, Senapati A, Tayal B et al. Myocardial Scar and Mortality in Chronic Aortic Regurgitation. J Am Heart Assoc 2020;9:e018731.
21. Musa TA, Treibel TA, Vassiliou VS et al. Myocardial Scar and Mortality in Severe Aortic Stenosis. Circulation 2018;138:1935-1947.
22. Everett RJ, Treibel TA, Fukui M et al. Extracellular Myocardial Volume in Patients With Aortic Stenosis. J Am Coll Cardiol 2020;75:304-316.
23. Singh A, Greenwood JP, Berry C et al. Comparison of exercise testing and CMR measured myocardial perfusion reserve for predicting outcome in asymptomatic aortic stenosis: the PRognostic Importance of MIcrovascular Dysfunction in Aortic Stenosis (PRIMID AS) Study. Eur Heart J 2017;38:1222-1229.

24. Bing R, Everett RJ, Tuck C et al. Rationale and design of the randomized, controlled Early Valve Replacement Guided by Biomarkers of Left Ventricular Decompensation in Asymptomatic Patients with Severe Aortic Stenosis (EVOLVED) trial. Am Heart J 2019;212:91-100.

25. Plana JC, Thavendiranathan P, Bucciarelli-Ducci C, Lancellotti P. Multi-Modality Imaging in the Assessment of Cardiovascular Toxicity in the Cancer Patient. JACC Cardiovasc Imaging 2018;11:1173-1186.

26. Patel AR, Kramer CM. Role of Cardiac Magnetic Resonance in the Diagnosis and Prognosis of Nonischemic Cardiomyopathy. JACC: Cardiovascular Imaging 2017;10:1180-1193.

27. Augusto JB, Johner N, Shah D et al. The myocardial phenotype of Fabry disease pre-hypertrophy and pre-detectable storage. Eur Heart J Cardiovasc Imaging 2020.

28. Lewis GA, Schelbert EB, Naish JH, Bedson E, et al. Pirfenidone in Heart Failure with Preserved Ejection Fraction-Rationale and Design of the PIROUETTE Trial. Cardiovasc Drugs Ther 2019;33:461-470.

29. Kim RJ, Fieno DS, Parrish TB, Al E. Relationship of MRI Delayed Contrast Enhancement to Irreversible Injury, Infarct Age, and Contractile Function. Circulation 1999;100:1992-2002.

30. McCrohon JA, Moon JCC, Prasad SK et al. Differentiation of heart failure related to dilated cardiomyopathy and coronary artery disease using gadolinium-enhanced cardiovascular magnetic resonance. Circulation 2003;108:54-59.

31. Kawel-Boehm N, Maceira A, Valsangiacomo-Buechel ER et al. Normal values for cardiovascular magnetic resonance in adults and children. J Cardiovasc Magn Reson 2015;17:29.

32. Kazmirczak F, Chen KA, Adabag S et al. Assessment of the 2017 AHA/ACC/HRS Guideline Recommendations for Implantable Cardioverter-Defibrillator Implantation in Cardiac Sarcoidosis. Circ Arrhythm Electrophysiol 2019;12:e007488.

33. Acosta J, Fernandez-Armenta J, Borras R et al. Scar Characterization to Predict Life-Threatening Arrhythmic Events and Sudden Cardiac Death in Patients With Cardiac Resynchronization Therapy: The GAUDI-CRT Study. JACC Cardiovasc Imaging 2018;11:561-572.

34. Khan FZ, Virdee MS, Palmer CR et al. Targeted left ventricular lead placement to guide cardiac resynchronization therapy: the TARGET study: a randomized, controlled trial. J Am Coll Cardiol 2012;59:1509-18.

35. Ramachandran R, Chen X, Kramer CM, Epstein FH, Bilchick KC. Singular value decomposition applied to cardiac strain from MR imaging for selection of optimal cardiac resynchronization therapy candidates. Radiology 2015;275:413-420.

36. Zghaib T, Ipek EG, Hansford R et al. Standard Ablation Versus Magnetic Resonance Imaging-Guided Ablation in the Treatment of Ventricular Tachycardia. Circ Arrhythm Electrophysiol 2018;11:e005973-e005973.

37. Chelu MG, King JB, Kholmovski EG, Al E. Atrial Fibrosis by Late Gadolinium Enhancement Magnetic Resonance Imaging and Catheter Ablation of Atrial Fibrillation: 5-Year Follow-Up Data. J Am Heart Assoc 2018;7:e006313-e006313.

38. Maron BJ, Maron MS. LGE Means Better Selection of HCM Patients for Primary Prevention Implantable Defibrillators. JACC: Cardiovascular Imaging 2016;9:1403-1406.

39. Kramer CM, Appelbaum E, Desai MY, Al E. Hypertrophic Cardiomyopathy Registry: The rationale and design of an international, observational study of hypertrophic cardiomyopathy. Am Heart J 2015;170:223-230.

40. Vermes E, Strohm O, Otmani A, Childs H, Duff H, Friedrich MG. Impact of the revision of arrhythmogenic right ventricular cardiomyopathy/dysplasia task force criteria on its prevalence by CMR criteria. JACC: Cardiovascular ImagingCardiovasc Imaging 2011;4:282-287.

41. Al-Khatib SM, Stevenson WG, Ackerman MJ, Al E. 2017 AHA/ACC/HRS Guideline for Management of Patients With Ventricular Arrhythmias and the Prevention of Sudden Cardiac Death: Executive Summary: A Report of the American College of Cardiology/American Heart Association Task Force on Clinical Practice Gui. J Am Coll Cardiol 2018;72:1677-1749.

42. Halliday BP, Gulati A, Ali A, Al E. Association Between Midwall Late Gadolinium Enhancement and Sudden Cardiac Death in Patients With Dilated Cardiomyopathy and Mild and Moderate Left Ventricular Systolic Dysfunction. Circulation 2017;135:2106-2115.

43. Guaricci AI, Masci PG, Muscogiuri G et al. CarDiac magnEtic Resonance for prophylactic Implantable-cardioVerter defibrillAtor ThErapy in Non-Ischaemic dilated CardioMyopathy: an international Registry. Europace 2021.

44. Trayanova NA, Pashakhanloo F, Wu KC, Halperin HR. Imaging-Based Simulations for Predicting Sudden Death and Guiding Ventricular Tachycardia Ablation. Circ Arrhythm Electrophysiol 2017;10.

45. Piers SR, Tao Q, de Riva Silva M, Al E. CMR-based identification of critical isthmus sites of ischemic and nonischemic ventricular tachycardia. JACC: Cardiovascular Imaging 2014;7:774-784.

46. Siebermair J, Suksaranjit P, McGann CJ, Al E. Atrial fibrosis in non-atrial fibrillation individuals and prediction of atrial fibrillation by use of late gadolinium enhancement magnetic resonance imaging. J Cardiovasc Electrophysiol 2019;30:550-556.

47. Puntmann VO, Carerj ML, Wieters I et al. Outcomes of Cardiovascular Magnetic Resonance Imaging in Patients Recently Recovered From Coronavirus Disease 2019 (COVID-19). JAMA Cardiol 2020.

48. Mangion K, Morrow A, Bagot C et al. The Chief Scientist Office Cardiovascular and Pulmonary Imaging in SARS Coronavirus disease-19 (CISCO-19) study. Cardiovasc Res 2020.

49. Kramer CM, Barkhausen J, Bucciarelli-Ducci C, Al E. Standardized cardiovascular magnetic resonance imaging (CMR) protocols: 2020 update. Journal of Cardiovascular Magnetic Resonance 2020;22:17-17.

50. Schulz-Menger J, Bluemke DA, Bremerich J et al. Standardized image interpretation and post-processing in cardiovascular magnetic resonance - 2020 update. Journal of Cardiovascular Magnetic Resonance 2020;22:19-19.

51. Neubauer S, Kolm P, Ho CY, et al. Distinct Subgroups in Hypertrophic Cardiomyopathy in the NHLBI HCM Registry. J Am Coll Cardiol 2019;74:2333-2345.

52. Geva T, Mulder B, Gauvreau K et al. Preoperative Predictors of Death and Sustained Ventricular Tachycardia After Pulmonary Valve Replacement in Patients With Repaired Tetralogy of Fallot Enrolled in the INDICATOR Cohort. Circulation 2018;138:2106-2115.

53. Ibanez B, Aletras AH, Arai AE et al. Cardiac MRI endpoints in myocardial infarction experimental and clinical trials: JACC scientific expert panel. J Am Coll Cardiol 2019;74:238-256.

54. Bulluck H, Hammond-Haley M, Weinmann S, Martinez-Macias R, Hausenloy DJ. Myocardial infarct size by CMR in clinical cardioprotection studies: insights from randomized controlled trials. JACC: Cardiovascular Imaging 2017;10:230-40.

55. Biomarkers Definitions Working G. Biomarkers and surrogate endpoints: preferred definitions and conceptual framework. Clin Pharmacol Ther 2001;69:89-95.

56. Messroghli DR, Moon JC, Ferreira VM et al. Correction to: Clinical recommendations for cardiovascular magnetic resonance mapping of T1, T2, T2* and extracellular volume: A consensus statement by the Society for Cardiovascular Magnetic Resonance (SCMR) endorsed by the European Association for Cardi. Journal of Cardiovascular Magnetic Resonance 2018;20:9-9.

57. Zou Z, Zhang HL, Roditi GH, Leiner T, Kucharczyk W, Prince MR. Nephrogenic systemic fibrosis: review of 370 biopsy-confirmed cases. JACC Cardiovascular imaging 2011;4:1206-1216.

58. Do DH, Eyvazian V, Bayoneta AJ et al. Cardiac magnetic resonance imaging using wideband sequences in patients with nonconditional cardiac implanted electronic devices. Heart rhythm 2018;15:218-225.

59. Walker S, Girardin F, McKenna C et al. Cost-effectiveness of cardiovascular magnetic resonance in the diagnosis of coronary heart disease: an economic evaluation using data from the CE-MARC study. Heart 2013;99:873-81.

60. Pletscher M, Walker S, Moschetti K et al. Cost-effectiveness of functional cardiac imaging in the diagnostic work-up of coronary heart disease. Eur Heart J Qual Care Clin Outcomes 2016;2:201-207.

61. Roifman I, Gutierrez J, Wang E et al. Evaluating a novel free-breathing accelerated cardiac MRI cine sequence in patients with cardiomyopathy. Magn Reson Imaging 2019;61:260-266.

62. Leiner T, Rueckert D, Suinesiaputra A et al. Machine learning in cardiovascular magnetic resonance: basic concepts and applications. J Cardiovasc Magn Reson 2019;21:61-61.

63. Bai W, Sinclair M, Tarroni G et al. Automated cardiovascular magnetic resonance image analysis with fully convolutional networks. Journal of Cardiovascular Magnetic Resonance 2018;20:65-65.

64. Fahmy AS, Rausch J, Neisius U et al. Automated Cardiac MR Scar Quantification in Hypertrophic Cardiomyopathy Using Deep Convolutional Neural Networks. JACC: Cardiovascular Imaging 2018;11:1917-1918.

65. Tat E, Bhatt DL, Rabbat MG. Addressing bias: artificial intelligence in cardiovascular medicine. Lancet Digital Health 2020;2:e635-e636.

Figure Legends

Figure 1 –Comprehensive stress perfusion CMR examination in a patient with multi-vessel coronary artery disease. A: Diastolic still frame image from short-axis cine MRI (SSFP). B: Corresponding gadolinium first-pass perfusion during adenosine infusion. The dark subendocardial rim demonstrates hypoperfusion in multiple coronary territories (white arrows). C: Corresponding LGE image following gadolinium contrast demonstrates a tiny rim of subendocardial enhancement (arrow) suggesting myocardial infarction in a territory of myocardium that demonstrates significant myocardial viability.

Figure 2 – CMR in Acute Myocardial Infarction. Apical short-axis image acquisition after gadolinium contrast demonstrating microvascular obstruction in a patient who presented with extensive myocardial injury due to anterior ST-elevation myocardial infarction. Microvascular obstruction is the region of hypoenhancement (dark zone, white arrow) surrounded by the large territory of enhancement.

Figure 3 – CMR in Valvular Heart Disease. In aortic regurgitation. (AR, left), cine sequences (A,D) are used to measure ventricular dimensions and systolic function as well as aortic valve morphology. A phase contrast sequence at the aortic valve level (B) is used to quantify the regurgitant fraction (C). The ascending aorta is also evaluated either with cine sequences (E) or with MR contrast angiography. In aortic stenosis (AS, center), cine sequences (F, I) are used to quantify ventricular dimensions and systolic function, and to planimeter the aortic valve area (G). Peak velocity at the aortic valve level is measured (H, J). LGE (K) and T1 mapping (L) sequences are usually included in the protocol to investigate the presence of focal and diffuse fibrosis. In mitral regurgitation (MR, right), cine sequences (M, N, Q) are used to quantify ventricular dimensions and systolic function, and to assess mitral valve morphology (N). Phase contrast sequences allow for the quantification of MR (P) and LGE sequences (R) are usually included in the protocol if coronary artery disease is suspected.

Figure 4 – CMR for Tissue Characterization in Cardiomyopathy. The examples demonstrate findings such as mid-myocardial LGE in a patient with genetic dilated cardiomyopathy due to a *LMNA* mutation (A), diffuse transmural LGE with altered gadolinium kinetics due to amyloid deposition in a patient with cardiac amyloidosis (B), anterior and lateral subepicardial LGE due to acute myocardial necrosis in a patient with acute myocarditis (C), multifocal subepicardial LGE due to a combination of acute and chronic myocardial damage in a patient with cardiac sarcoidosis (D), elevated T_1 (1180 ms) on pre-contrast T_1 mapping in a patient with cardiac amyloidosis (E), elevated extracellular volume fraction (68%) on post-contrast T_1 mapping in a patient with cardiac amyloidosis (F), anterior and lateral subepicardial elevated T_2 (59 ms) on T_2 mapping in a patient with acute myocarditis (G). and decreased T_2* (5.2 ms) on T_2* mapping in a patient with iron overload cardiomyopathy (H).

Figure 5 – CMR for 3D Strain and Scar Visualization for Cardiac Resynchronization Therapy and Ventricular Tachycardia Ablation. In a patient undergoing cardiac resynchronization therapy, the area of latest activation based on CMR DENSE relative to the implanted quadripolar lead is shown in red (A), and an overlay of scar and coronary venous anatomy on the 3D contour and quadripolar lead is also shown (B). A three dimensional map from CMR demonstrating key sites for ventricular tachycardia ablation based on scar is also shown (C).

Table 1: Key structural and physiologic CMR endpoints

	Underlying pathophysiology	Relation to other imaging modalities	Relation to other biomarkers	Relation to hard endpoints	comments
Volumes	Nonspecific	CMR is more accurate and reproducible, requiring significantly fewer patients in comparison to echocardiography or radionuclide ventriculography to achieve the same power		Strong relationship if highly abnormal, weak relationship if mildly abnormal	
Ejection Fraction	Nonspecific	CMR is more accurate and reproducible, requiring significantly fewer patients in comparison to echocardiography or radionuclide ventriculography to achieve the same power			
Strain	Nonspecific	Similar to echocardiographic speckle tracking. In comparison to echocardiography more influenced by endocardium, lower temporal resolution, better visualization of inferior wall and right ventricular free wall.	More sensitive for abnormalities than volumes or ejection fraction		Regional function still difficult. Global longitudinal strain was most reproducible.
LGE	Specific for cardiac damage and the only non-invasive technique to demonstrate direct correlation with	Higher spatial resolution than SPECT or PET, straightforward combination with wall motion. Reference	Long term marker of myocardial damage. Stronger marker of outcome than volumes,	Strong relationship to hard endpoints. Any increase of LGE burden	Absolute quantification influenced by timing, contrast dose, diffuse fibrosis, and

	histopathology. Chronic: focal replacement fibrosis. Acute: focal necrosis and edema	standard for focal scar.	ejection fraction or strain.	increases event rate.	method of quantification.
Perfusion	Specific for myocardial ischemia. Epicardial and microvascular damage can be separated	Higher spatial resolution than SPECT or PET, thus, better detection of subendocardial abnormalities. Quantification possible.	Provides direct information on myocardial flow rather than indirect via coronary anatomy or pressure	Strong relationship to hard endpoints. Any increase of ischemia increases event rate.	
Mapping	Specific for myocardial water content (T2), strongly correlated to diffuse myocardial fibrosis (T1, extracellular volume fraction) and myocardial iron accumulation ($T2^{*}$)	No other imaging modalities available	Provides a direct assessment of myocardial damage. Can partially be obtained with myocardial biopsy.	Strong relationship to hard endpoints	Strict locking of sequence parameters required for native scans.
Vascular function	Pulse wave velocity / aortic distensibility	No other imaging modalities	Provides an assessment of vascular stiffness and compliance	Mechanistic outcome	Cine and/or phase contrast methods

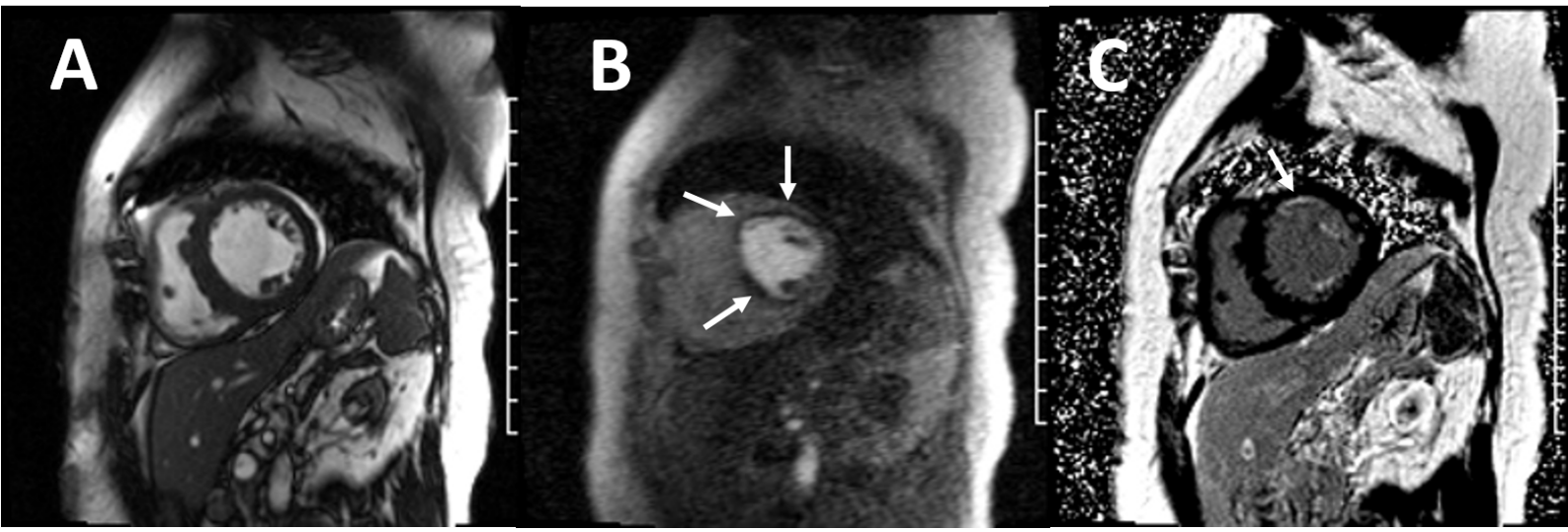
A
B
C

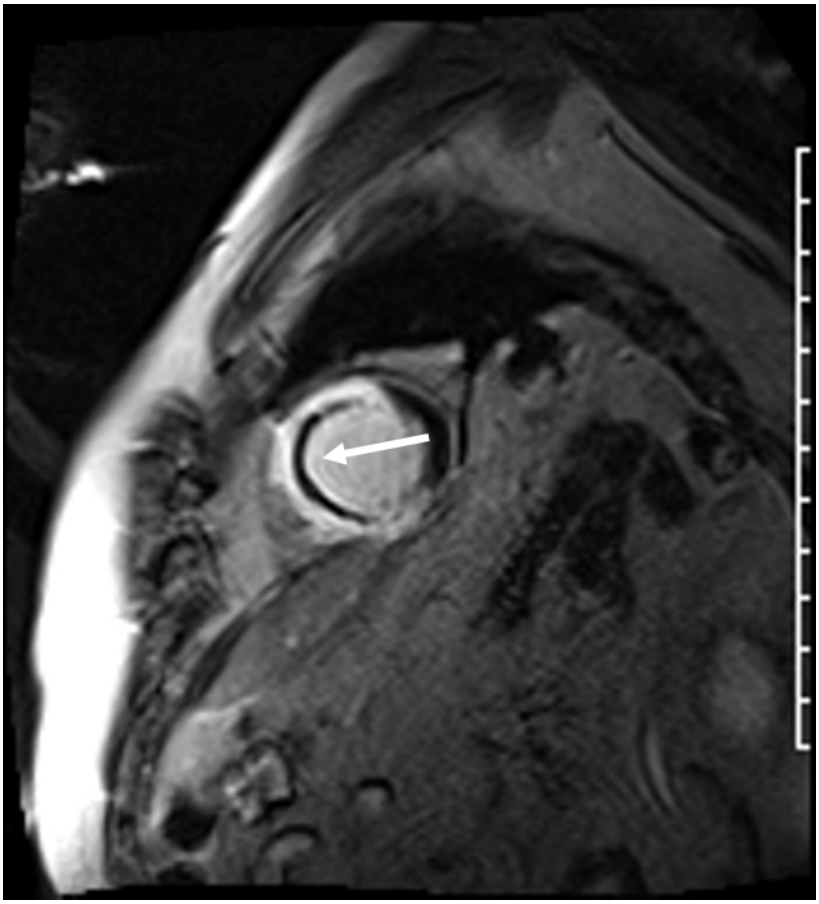

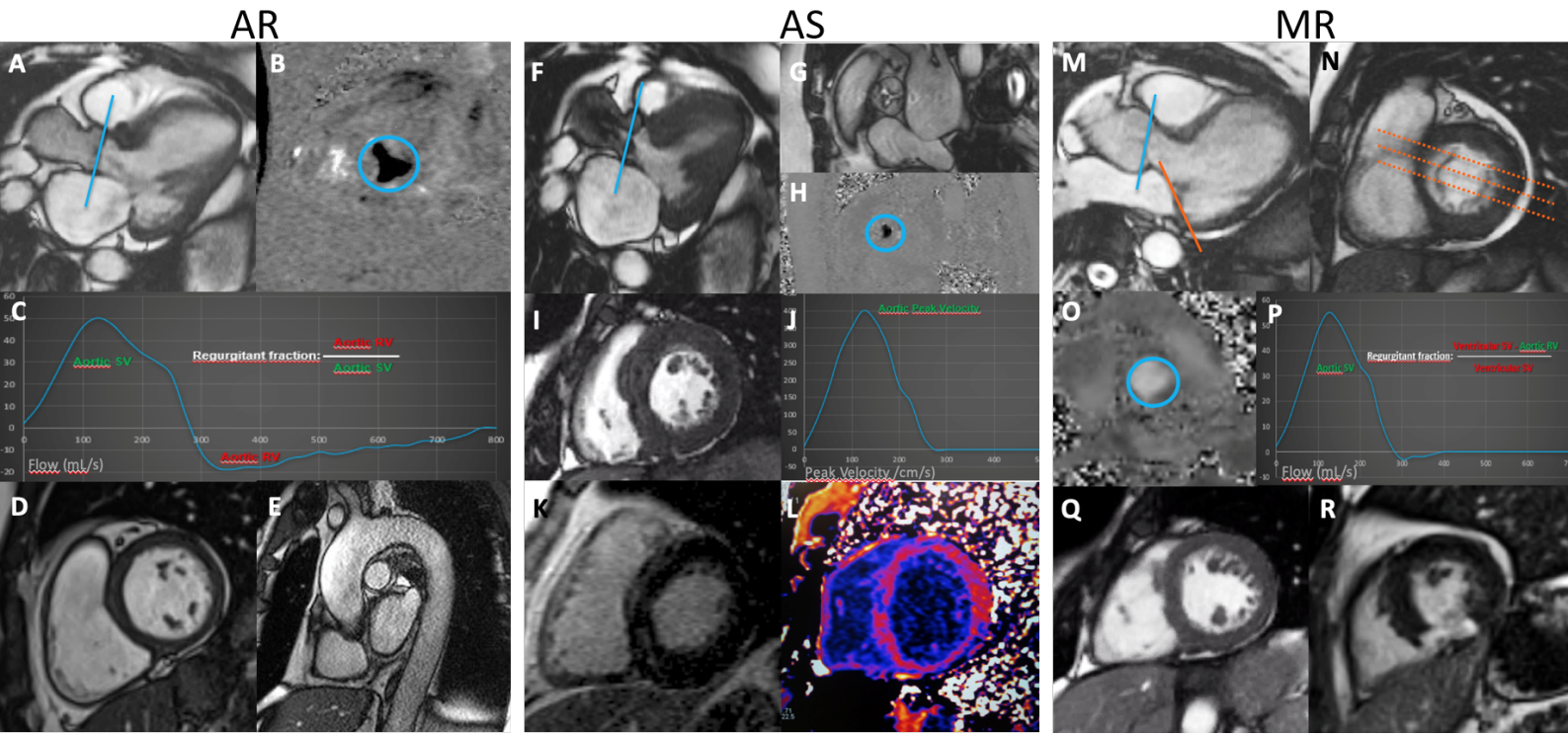
AR
AS
MR
A
B
C
D
E
F
G
H
I
J
K
L
M
N
O
P
Q
R
Aortic SV
Regurgitant fraction:
Aortic RV
Aortic SV
Flow (mL/s)
Aortic RV
Aortic Peak Velocity
Peak Velocity (cm/s)
Aortic SV
Regurgitant fraction:
Ventricular SV - Aortic RV
Ventricular SV
Flow (mL/s)

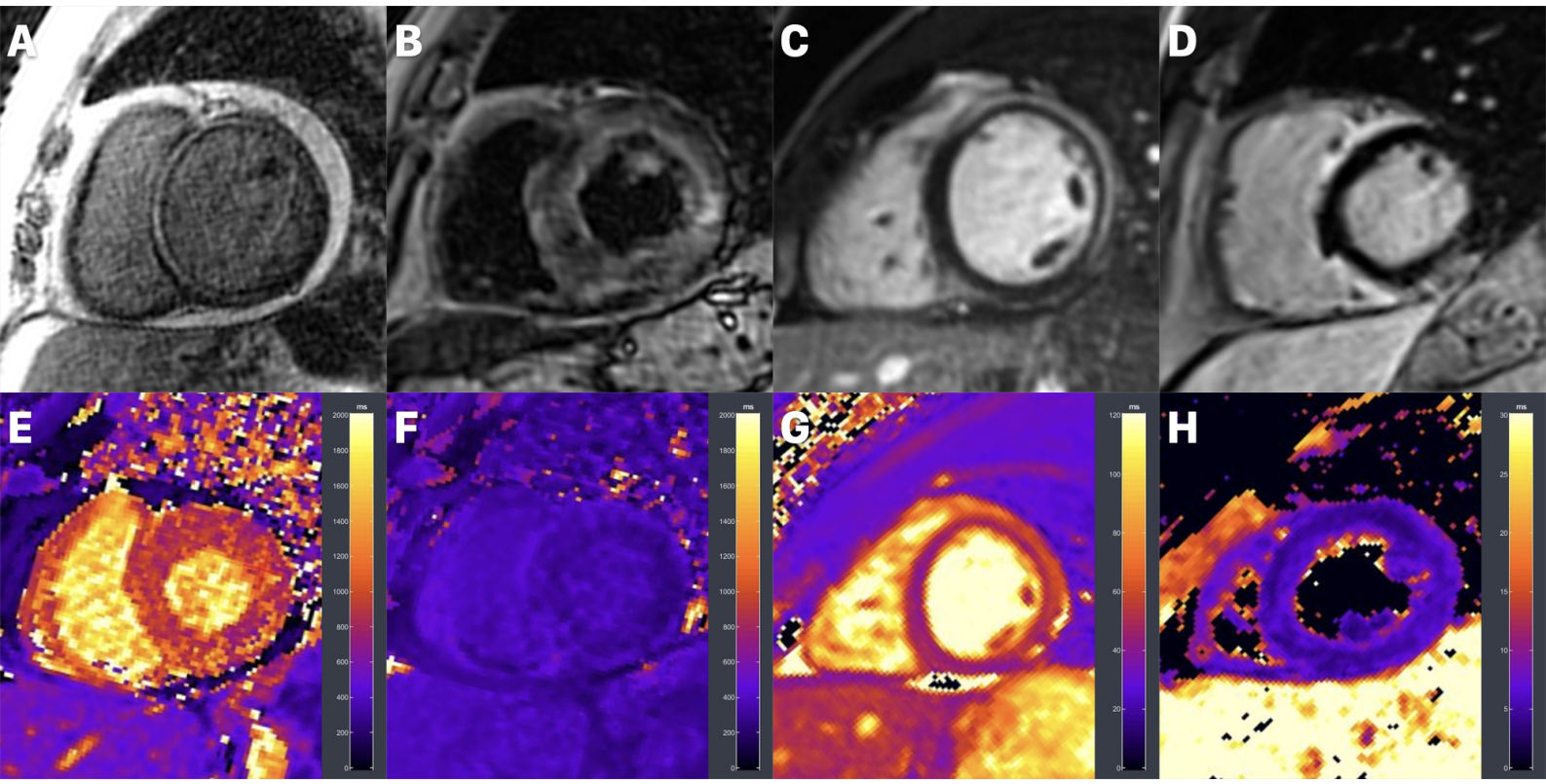
A
B
C
D
E
F
G
H
ms
2000
1800
1600
1400
1200
1000
800
600
400
200
0
120
100
80
60
40
20
30
25
20
15
10
5

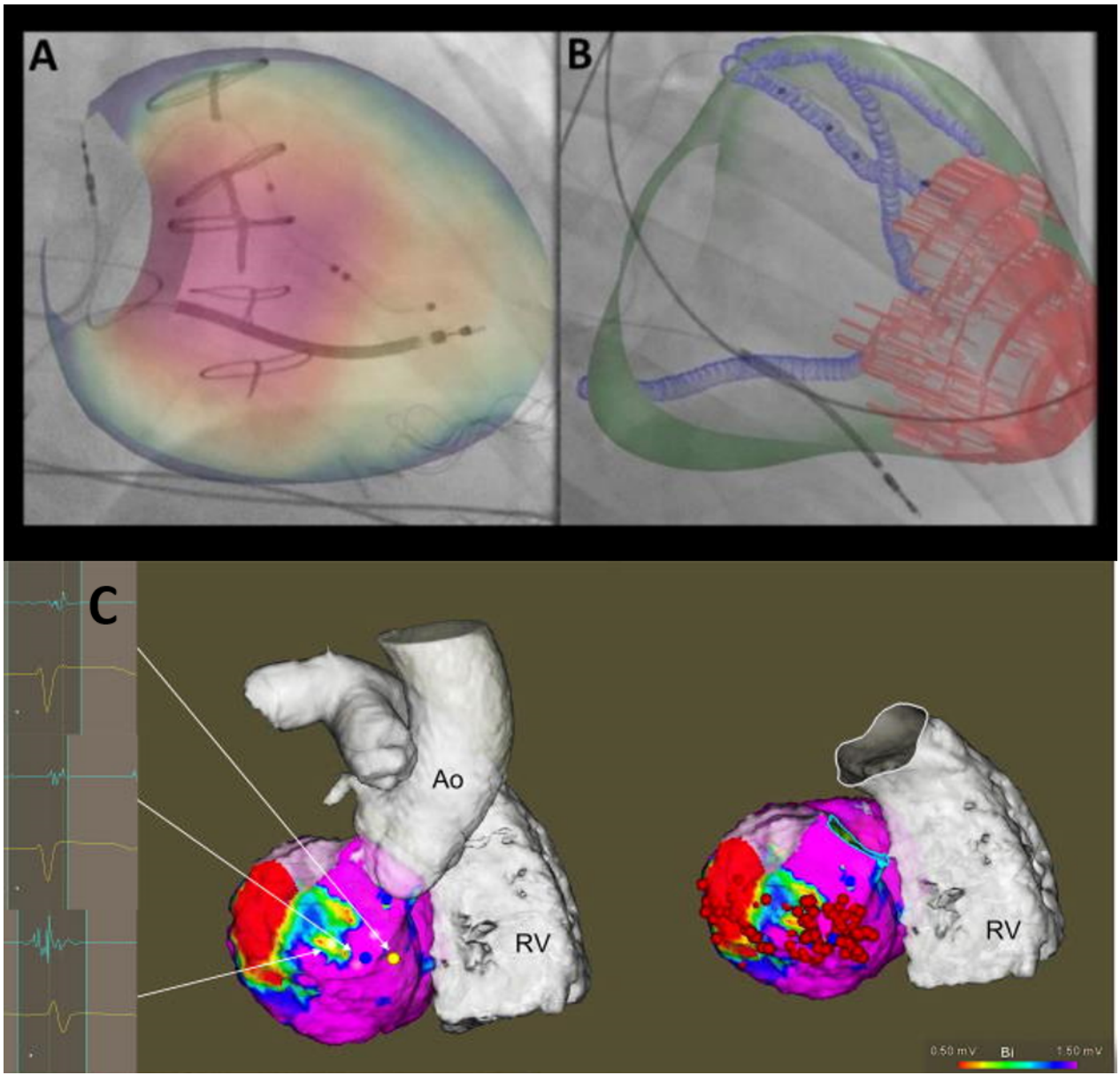
A
B
C
Ao
RV
RV
0.50 mV
Bi
1.50 mV

Supplementary Table Summarizing Status of Publications in CMR in Areas with Unmet Needs					
Study	Study Type	N	Method(s) of Assessment	Outcome	Findings
Coronary Artery Disease					
GadaCAD(1)	RCT	764	Vasodilator stress CMR	Diagnostic accuracy for detection of CAD	CAD prevalence 27.8% determined by QCA stenosis >70%
					Single vessel QCA stenosis >70%: Sensitivity 78.9%, specificity 86.8%, AUC 0.871.
					Multivessel CAD detection: Sensitivity 87.4%, specificity 73%;
					Single vessel QCA stenosis >50%: Sensitivity 64.6%, specificity 86.6%
Heitner et al.(2)	Observational	9,151	Vasodilator stress CMR	Death	Vasodilator stress CMR is associated with death in patients with known or suspected CAD as well as in multiple subpopulations defined by history of CAD and LVEF.
SPINS Registry(3)	Observational	2,349	Vasodilator stress CMR	Cardiac death and non-fatal MI; downstream imaging and procedural costs	Abnormal CMR (ischemia or LGE) corresponds to 4-fold increased rate of cardiac death or MI in first year. Normal CMR associated with negative event rates of approximately 99% over 5 years, and low costs spent on cardiac investigations
STRATEGY(4)	Observational	600	CTCA vs stress CMR	MACE	Stress CMR strategy – lower MACE (5% vs 10%, p<0.01) and cost effectiveness ratio (119.98 vs 218.12 Euro/y; p<0.001) compared to CTCA; Less downstream non-invasive testing, ICA, and revascularization procedures.
MR-IMPACT II (5)	RCT	533	Vasodilator Stress CMR vs. SPECT	Diagnostic performance of stress CMR vs. SPECT	Prevalence of CAD 49%; CMR sensitivity 0.67, specificity 0.61; SPECT sensitivity 0.59 specificity 0.72
EURO-CMR Registry(6)	Observational	3647	CMR vs ICA with/without CFR	Cardiac death and Non-fatal MI	Annualized event rate for normal stress CMR 0.38%
				Cost analysis	Substantial cost reduction in CMR+ICA strategy (14-34%) vs. ICA+FFR strategy
MR-INFORM(7)	RCT	918	Stress CMR- vs. FFR-based management strategy	Revascularization	Fewer downstream revascularizations in CMR-strategy 35.7% vs. 45.0% FFR-group (p=0.005)
				Primary (MACE at 12 months)	3.6 % for CMR-group vs. 3.7% for FFR-group
				Angina at 12-months	49.2% CMR-group vs. 43.8% FFR-group angina free (p=0.21)

CE-MARC(8)	RCT	752	Stress CMR vs. SPECT vs. ICA	Diagnostic accuracy of CMR and SPECT to detect significant CAD as determined by ICA	Significant CAD by ICA in 39% of patients
					CMR sensitivity 86.5%, specificity 83.4%, positive predictive value 77.2%, negative predictive value 90.5%
					SPECT sensitivity 66.5%, specificity 82.6%, positive predictive value 71.4%, negative predictive value 79.1%.
CE-MARC2(9)	RCT	1202	Stress CMR vs. SPECT vs. NICE Guidelines	Unnecessary coronary angiography	CMR vs. NICE OR 0.21 (p<0.001)
					CMR vs. SPECT OR 1.27 (p=-0.32)
				MACE	CMR vs NICE OR 1.36 (p=0.52)
					CMR vs SPECT OR 0.95 (p=0.88)
Greenwood et al. (10)	Observational	744	Stress CMR, SPECT, ICA	5-year MACE	16% had at least 1 MACE
					Abnormal CMR findings were strong, independent predictors of MACE (HR 2.77, p<0.001)
					CMR remained sole independent predictor of MACE after adjustment for cardiovascular risk factors, angiography findings, or pre-test risk stratification for initial treatment.
Walker et al. (11)	Observational		ETT, SPECT, CMR, and ICA	Costs; health outcomes in quality-adjusted life-years (QALYs)	Most cost effective stretegies at UK NICE accepted cost-effectiveness thersholds: 1. Strategy 3: ETT, followed CMR if ETT is positive or equivocal followed by ICA if CMR is positive or inconclusive 2. Strategy 5: CMR followed by ICA if CMR is positive or equivocal
					Strategy 3 is coest effective at lower end of threshold range by UK standards (£20 000 per QALY gained)
					Strategy 5 is cost effective at the higher end of threshold range by UK standards (£30 000 per QALY gained)
Eitel et al.(12)	Observational	1235	CMR-Feature Tracking	MACE 12 months after MI	Global longitudinal strain added incremental prognostic value for all-cause mortality above LVEF (C-index increase from 0.65 to 0.73, p=0.04) and infarct size (c-index increase from 0.6 to 0.78; p=0.002)
Rijlaarsdam-Hermsen et al. (13)	Observational	642	Vasodilator stress CMR -only	Stress-only perfusion CMR after CAC>0 improved diagnostic yield of ICA	Obstructive CAD in 12%; Adenosine-CMR sensitivity was 90.9%;, specificity 98.7%, positive predictive value 92%, negative predictive value 98.6%

CvLPRIT-CMR(14)	RCT	205	Infarct size, myocardial salvage index	Infarct size measured by CMR; Secondary measures: MVO, myocardial salvage index, and final infarct size 9 months post STEMI	No difference in total infarct size, ischemic burden, LV volumes between complete revascularization vs. infarct related artery revascularization treatment groups at follow-up CMR
PROSPECT(15)	Observational	209	LVEF, myocardial salvage index, MVO, myocardial hemorrhage	MACE	CMR score (HR 1.86, p<0.001) was independently associated with MACE. CMR score provides incremental prognostic stratification as compared with GRACE score and TTE-EF
OMEGA-REMODEL(16)	RCT	358	LVEF, LGE		Treatment of AMI with high-dose omega-3 fatty acids was associated with reduction in LV remodeling, noninfarct fibrosis and serum biomarkers of inflammation.
McCartney et al. (17)	RCT	440	LGE	MACE	No difference in mean MVO between 20-mg Alteplace vs. placebo groups (3.5% vs. 2.3%, p=0.32) nor compared to the 10-mg Alteplace vs. placebo group (2.6% vs. 2.3%; p=0.74)
					MACE: 15 patients (10.1%) in the placebo group, 12 (8.2%) in the 20-mg alteplase group, 18 (12.9%) in the 10-mg alteplase group
Nazir et al.(18)	RCT	247	LGE	Infarct size % LV Mass	High-dose IC adenosine and SNP during primary PCI in the setting of STEMI (single-vessel disease, presenting within 6 hours of symptom onset) did not reduce infarct size (%LV mass) or MVO by CMR compared to standard PCI.
					Infarct size (12.0 vs. 8.3, p=0.031), MACE at 30 days (HR 5.39, p=0.04) and 6 months (HR=6.53, p=0.01) was higher and ejection fraction reduced in the adenosine treated group control (42.5 ±7.2% vs. 45.7 ± 8%, p=0.027) .
Piccolo et al. (19)	Observational	2470	CMR myocardial salvage index	1-year composite death or reinfarction	Prevalence of diabetes 19% vs. 81% controls;
					Primary endpoint was significantly less in diabetic patients randomized to intracoronary abciximab compared to IV bolus (9.2% vs. 17.6%, HR 0.49, p=0.009)
					Intracoronary vs. IV abciximab was associated with significantly lower risk of mortality (5.8% vs. 11.2%, HR 0.51,p=0.043) and definite/probable stent thrombosis (1.3% vs. 4.8%; HR 0.27, p=0.046)
					Myocardial salvage index by CMR was significantly increased only in diabetic patients receiving intracoronary vs. IV abciximab (54.4 vs. 39.0, p=0.011)
Microvascular disease (ANOCA)					
Thomson et al. (20)	Observational	118	Stress perfusion CMR + invasive microvascular function testing (CFR)		No difference in qualitative analysis of CMR perfusion studies Reduced global MPRi in ANOCA compared to controls (1.79 vs. 2.23, p<0.0001)

					MPRi threshold of 1.84 predicted abnormal invasive CFR (sensitivity 73%; specificity 74%)
Williams et al.(21)	Observational	54	Semiquantitative perfusion CMR, IMR, hMR		Modest correlation of CMR-derived MPRi with hMR (r=0.58, p<0.001) but not IMR (r=-0.27, p=0.15)
Zorach et al.(22)	Observational	46	Quantitative stress CMR	Myocardial perfusion and myocardial perfusion ratio	Stress myocardial perfusion (2.65 vs. 3.17 ml/min/g) and MPR (2.21 vs. 2.93) were lower compared to controls
Kotecha et al.(23)	Observational	50	Quantitative stress CMR	Quantitative MBF and MPR with FFR and IMR	FFR positive regions had reduced MBF (1.47ml/g/min) and MPR (1.75) compared to FFR negative regions (MBF 2.1 ml/g/min; MPR 2.41) where there was MVD (IMR-positive) Stress MBF ≤ 1.94 ml/g/min was accurate to detect obstructive CAD in a regional pattern (AUC 0.9, p<0.001).
Non-ischemic Cardiomyopathy					
MyoRacer-Trial(24)	Observational	129	T1 and T2 mapping	AUC	Acute symptoms: Native T1 (AUC 0.82), T2 (0.81), ECV (0.75), LLC (0.56)
					Chronic symptoms: T2 AUC 0.77
					T1 and T2 mapping useful in the diagnosis of myocarditis and are superior to LLC in acute setting. Only T2 useful in chronic setting.
Leong et al.(25)	Observational	68	LGE-CMR	Change in LVEF over time	Extent of CMR-LGE in DCM showed independent association with failure of EF response to medical therapy in newly diagnosed DCM
Gulati et al.(26)	Observational	472	LGE	All-cause mortality Secondary endpoints: CV mortality or cardiac transplantation; Arrhythmic composite of SCD or aborted SCD	Midwall LGE and LGE extent associated with all-cause mortality, CV mortality, transplant, SCD composite, and HF after adjustment for LVEF
Puntmann et al.(27)	Observational	637	T1 mapping and LGE	All-cause mortality; Secondary endpoint: HF mortality and hospitalization	Native T1 and LGE were predictive of all-cause mortality and HF composite endpoint in non-ischemic dilated cardiomyopathy
Hypertrophic Cardiomyopathy					
Weng et al.(28)	Observational	2993	LGE	SCD, all-cause mortality, CV mortality	+LGE associated with increased risk for SCD (OR 3.41, p<0.001), all-cause mortality (OR 1.8, p=0.004), and CV mortality (OR 2.93, p=0.001)
Neubauer et al. (29)	Observational	2755	LGE, T1 mapping, ECV		Isolated basal septal hypertrophy (46%); Reverse septal curvature (38%); Apical HCM (8%); Concentric HCM (1%); Mid-cavity obstruction+apical aneurysm (3%); Other (1%)
					50% were LGE+; mean LGE mass 3.7 ±5.2% of LV mass; Reverse septal curvature associated with 79% of cases with >10% LGE
Chan et al.(30)	Observational	1293	LGE	SCD events	LGE extent ≥15% of LV mass associated with 2-fold increase in SCD events (HR 1.46/10% increase in LGE, p=0.002)

Dass et al.(31)	Observational	58	Native T1 and LGE	Native T1 and LGE compared to normal	In HCM and DCM, native T1 mapping is abnormal beyond LGE
Hinojar et al.(32)	Observational	164	Native T1 and ECV		Native T1 can discriminate between patients with HCM and hypertension
Puntmann et al.(33)	Observational	52	Native T1 and ECV		Native T1, post-contrast T1, and ECV indices can be used to accurnately discirminate between normal and diseased myocardium in HCM and DCM
Ho et al.(34)	Observational	77	ECV		HCM sarcomere mutation carriers have increased ECV even when LVH is absent.
Mclellan et al.(35)	Observational	100	Post-contrast T1		Post-contrast T1 was associated with non-sustained VT in HCM
Left Ventricular Non-compaction					
Kawel et al.(36)	Observational	1000	Trabeculated/Compacted Myocardium ratio >2.3		The ratio of trabeculated/compacted myocardium > 2.3 was found in 43% (140/343) of participants without CV disease or hypertension.
Weir-McCall et al.(37)	Observational	1480	LAX, SAX LVNC ratio; noncompaction ratio ≥2 SAX systolic and diastolic ratio→ + quantification of noncompacted and compacted myocardial mass ratios	Number of criteria met	14.8% met ≥1 diagnostic criteria 7.9% met 2 criteria 4.3% met 3 criteria 1.3% met all 4 criteria for LVNC
Jacquier et al.(38)	Observational	16	LV volumes, ejection fraction and trabeculated LV mass		Trabeculated LV mass over 20% of global LV mass predicted LVNC (sensitivity 93.6% and specificity of 93.7%)
Andreini et al.(39)	Observational	113	Noncompacted/compacted ratio >2.3; LVEF; RVEF, LGE	Cardiac events (HF hospitalizations, cardiac deaths, VA, thromboembolic events)	Degree of LV trabeculation in LVNC did not have incremental prognostic value over LV dilation, systolic dysfunction and +LGE.
Muscular Dystrophies					
Hor et al.(40)	Observational	70	CMR tagging		Myocardial strain abnormalities are prevalent in DMD patients <10 years-old and decline with advanced age; Reduced EF and positive MDE exhibited the lowest strain measures.
Becker et al.(41)	Observational	63	LGE, LVEF		LGE positive MD patients showed more frequently reduced LVEF and elevated hs-Trop level
Hor et al.(42)	Observational	314	LV volumes; LVEF; LGE		LGE prevalence is 36% and increases with age; 84% of LVEF<55% had LGE compared to 30% with LVEF>55%; 10% of LGE+ patients died on average follow-up of 11 months.
Tandon et al.(43)	Observational	98	LVEF; LGE		LVEF declined on average 2.2±0.31% annually when LGE is present and 0.93±0.09% for each LGE+ segment.
Taylor et al.(44)	RCT	25	LGE		Intracoronary CAP-1002 in DMD demonstrates significant scar size reduction (LGE) and improvement in inferior systolic thickening compared to control.

Cardiac Amyloidosis					
Martinez-Naharro et al. (45)	Observational	134	Native T1, ECV	Mortality	Native T1 (HR 1.225 per 59ms increase) and ECV (1.155 per 3% increase)in wild-type ATTR predicted death over a mean follow-up of 32±17 months. Only ECV was independently predictive after multivariable adjustment.
Martinez-Naharro et al.(46)	Observational	31	ECV, LGE		ECV reduction (regression) occurred in 13/31 (42%) with prevalence higher in patients with complete/very good hematologic response.
Fontana et al.(47)	Observational	257	ECV, total cell volume		ECV measures are higher in mutant (0.6) and wild-type (0.57) ATTR vs. AL (0.54) amyloidosis
Kotecha et al.(48)	Observational	286	T2 mapping		T2 is higher in untreated AL amyloid compared to treated AL and ATTR, and independent predictor of death even after adjustment for ECV and nt-pro-BNP (HR 1.32, CI 1.05-1.67)
Banypersad et al.(49)	Observational	100	T1 mapping; ECV	Mortality	ECVi was raised in systemic amyloidosis and independently predicted mortality (HR 4.41, CI 1.35-14.4) after adjusting for E:E', EF, diastolic dysfunction grade, and NT-proBNP
Fontana et al.(50)	Observational	270	Native T1 mapping		T1 elevated in ATTR compared with HCM and normal subjects ($p<0.0001$) but not as high as in AL amyloidosis.
Karamitsos et al.(51)	Observational	106	Native T1 mapping; LGE		Native T1 cutoff of 1020ms resulted in 92% accuracy for identifying cardiac involvement in AL amyloidosis.
Banypersad et al.(52)	Observational	60	ECV		Mean ECV was significantly elevated in patients with Al amyloidosis (0.4) compared to controls (0.25) $p<0.001$
Fontana et al.(53)	Observational	250	LGE, ECV, T1 mapping		ECV tracked increasing amyloid burden with subendocardial LGE (ECV 0.4-0.43 in AL; 0.39-0.4 in ATTR) to transmural (0.48-0.55 in AL; 0.47-0.59 in ATTR); 27% mortality with transmural LGE (HR 5.4, $p<0.0001$) predicting death even after adjustment (HR 4.1, $p<0.05$).
White et al.(54)	Observational	154	Visual T1 assessment; LGE	All-cause mortality	LGE was the most important predictor of death in suspected cardiac amyloidosis (HR 5.5, $p<0.0001$); Comparing LGE to histology, sensitivity (93%), specificity (70%), and accuracy (84%).
Cardiac Siderosis					
Kirk et al.(55)	Observational	652	Myocardial T2*		Relative risk of arrhythmia for cardiac T2*<20ms was 4.6 (CI 2.66-7.95)

Leonardi et al.(56)	Observational	24	Myocardial T2*		Increased myocardial iron by T2* was strongly associated with lower LVEF (T2*<9 ms sensitivity of 100%, specificity of 89% for EF <50%)
Modell et al.(57)	Observational	850	Myocardial T2*		Reduction in rate of death from 7.9 to 2.3 deaths per 1000 patient years likely attributable to T2* CMR diagnosis of siderosis guiding iron chelation and treatment
Anderson et al.(58)	Observational	106	Myocardial T2*		Inverse correlation between iron concentration by biopsy and liver T2* (R=0.93, p<0.001); All ventricular dysfunction had myocardial T2* of <20ms and was the most significant variable to predict requirement for cardiac medication
Anderson et al.(59)	Observational	7	LVEF, LVEDVI, LVESVI, LVMass index, myocardial and liver T2*		After IV desferrioxamine treatment 6/7 siderosis patients showed progressive improvement in myocardial T2*, LVEF, LV volumes, and LV mass index.
Anderson et al.(60)	Observational	45	Myocardial T2*, LVEF		Deferiprone group demonstrated significantly less myocardial iron (34ms vs 11.4ms, p=0.02) comared to desferrioxamine treated controls with thalassaemia major.
Tanner et al.(61)	Observational	167	T2*; LVEF		Deferoxamine and deferiprone combination treatment reduced myocardial iron and improved EF in thalassemia major patients with mild-moderate cardiac siderosis
Valvular Heart Disease					
Singh et al. (62)	Observational	174	Adenosine stress CMR ETT Echocardiography	Composite: typical AS symptoms requiring referral for AVR + CV death + MACE	27% patients reached primary outcome over median follow-up 374 days; Mean MPR was 2.06 ± 0.65 in primary outcome group vs. 2.34 ±0.7 (p=0.022) reference group
					Moderate association between MPR and primary outcome (AUC 0.61, p=0.02) but not superior to ETT (AUC 0.59, p=0.027).
Cavalcante et al.(63)	Observational	578	Myocardial infarction size by LGE (MIS), Ischemic Mitral Regurgitation (IMR),	Death or cardiac transplant	Interaction of IMR severity and MIS was a strong predictor of adverse outcomes (P=0.008)
Uretsky et al.(64)	Observational	103	MR severity echo vs. CMR		Strong correlation between post-surgical LV remodeling and MR severity by MRI (r=0.85, p<0.0001), no correlation with echo-based MR assessment (r=0.32, p=0.1)
Everett et al. (65)	Observational	440	ECV, T1 mapping, LGE	CV and all-cause mortality	ECV% independently correlated to LGE and lower LVEF (p<0.05)
					Incremental increase in all-cause mortality seen across ECV% tertiles (17.3, 31.6, 52.7 deaths per 1000 patient-years; p=0.009)
					ECV% associated with CV mortality (p=0.003) and indepedently associated with all-cause mortality after adjustment for age, gender EF, and LGE (HR per % increase in ECV%: 1.10, p=0.013).

Loudon et al.(66)	Observational	110	LGE		Osteoprotegerin levels in patients with AS and chronic MI were higher than those without fibrosis (p=0.005)
Ahn et al.(67)	Observational	117	Stress CMR in AS		MPRI values significantly lower in severe AS without obstructive CAD compared to controls
Biederman et al.(68)	Observational	24	LVMass index (LVMI); EF, LVEDVi		LVMI, EF, LVEDVi, and LVSV improved post-AVR by 6 months follow-up
PINOT NOIR(69)	Observational	16	Pulmonic regurgitant fraction post iNO		iNO administered during CMR appeared to reduce regurgitant fraction with at least moderate PI
Dweck et al.(70)	Observational	91	Planimetry; velocity mapping, LVMi, LV volumes, LVmass/volume		Severity of AS was unrelated to the degree and pattern of hypertrophy in AS
Baron-Rochette et al.(71)	Observational	154	LGE	Mortality	+LGE predicted increased post-operative mortality (OR 10.9, p=0.02) and decreased all-cause survival (73% vs. 88%, p=0.02) and cardiovascular survival (85% vs. 95%, p=0.03) post surgical AVR. LGE (HR3.2, p<0.01) and NYHA Class III/IV were sole independent predictors of all-cause mortality after surgical AVR.
Rajesh et al. (72)	Observational	109	LGE	Mortality	43% of AS had +LGE predicted hospitalization for heart failure (OR 3.8, p=0.01) and drop in LVEF (OR 5.8, p=0.005) but not mortality.
Musa et al. (73)	Observational	674	LGE	Cardiovascular and all-cause mortality	51% +LGE in AS; Each 1% increase in LGE associated with 8% increase in cardiovascular mortality (HR 1.08, p<0.001) and 11% increase in all-cause mortality (HR1.11, p<0.001) regardless of surgical vs. transcatheter AVR.
Chin et al. (74)	Observational	166	LGE, iECV, T1	Mortality	Midwall LGE prevalence in AS was 27;LGE and iECV demonstrated a graded increase in unadjusted all-cause mortality (p=0.009)
Lee et al. (75)	Observational	127	Native T1, LGE	All-cause mortality + hospitalization for heart failure	Native T1 values were increased in AS; Over median 27.9 months, LGE and native T1 measurements were associated with to all-cause death and hospitalization for heart failure.
Kang et al.(76)	RCT	302	Planimetered MVA		No significant differences in achieved MVA by either Inoue and double-balloon techniques
Treibel et al.(77)	Observational	181	ECV, matrix volume (LV mass x ECV), cell volume (LV mass x [1-ECV])		Post-AVR, focal fibrosis does not resolve, but diffuse fibrosis and myocardial cellular hypertrophy regress which correlate with structural and functional improvements.

Myerson et al.(78)	Observational	113	AR regurgitant fraction; EDV		Regurgitant fraction by CMR >33% progressed to surgery within 3 years (AUC 0.93, p<0.0001)
Myerson et al. (79)	Observational	199	MR regurgitant fraction; EDV		91% of asymptomatic mitral regurgitation patients with regurgitant volume ≤ 55ml survived without surgery for 5 years vs. 21% with regurgitant volume ≥ 55 ml (p<0.0001)
					Optimal cutoff for MR regurgitant fraction was 40% and 100mL/m^2 for LVEDVi
Chaikriangkrai et al.(80)	Observational	48	LGE	Adverse clinical events	+LGE 40% of chronic MR patients; LGE independently associated with post-operative adverse clinical events (HR 4.775, p=0.037) after MV repair.
Azevedo et al. (81)	Observational	54	LGE	LVEF recovery	LGE demonstrated inverse correlation with degree of left ventricular functional improvement after MV surgery; LGE extent was independently associated with all-cause mortality.
Heart Rhythm Disorders					
CAMERA-MRI(82)	RCT	68	LVEF, LGE	LVEF improvement	Absolute LVEF improved by 18% in the catheter ablation group compared to 4.4% in medical rate control group
Paetsch et al.(83)	Observational	30	Whole heart, T2-weighted, early/late gadolinium enhancement		CMR-guided EP typical right atrial flutter ablation demonstrates similar safety and efficacy as fluoroscopy-guided flutter ablation.
Bilchick et al.(84)	Observational	100	DENSE Strain	Death, heart transplantation, LVAD or appropriate ICD therapies	47% reached primary clinical endpoint; 18% had appropriate ICD therapies median f/u 5.3 years
					Combined clinical and strain model demonstrated improved AUC at 2 years (0.76) and 4 years (0.75) compared to each individual model.
Klem et al.(85)	Observational	137	LVEF + LGE	Death or appropriate ICD discharge for sustained VT	Scar size >5% was an independent predictor of outcome
Halliday et al.(86)	Observational	399	LGE	SCD or aborted SCD	17.8% with +LGE reached endpoint compared to 2.3% -LGE (p<0.0001)
Levya et al.(87)	Observational	559	LGE	CV death, or CV death+ HF hospitalization	CMR guided LGE+ patients had the highest risk of CV death (HR6.34), CV death+HF hospitalization (HR 5.57) and death from any cause or hospitalizations for MACE (HR 4.74) compared to CMR guided LGE- patients (p<0.0001).
Levya et al. (88)	Observational	258	LGE	CV death; MACE	Midwall LGE independently predicted CV mortality (HR 18.6, p=0.0008), MACE mortality or hospitalization (HR 7.57, p<0.0001), and CV mortality or HF hospitalization (HR 9.56, p=0.0004) in patients undergoing CRT DCM + midwall LGE had similar outcome to ICM
ARVC					

Vermes et al.(89)	Observational	294	RV dilation (global or segmental); RV microaneurysm; RV regional hypokinesis vs. Combined severe regional abnormalities with global RV dilation or dysfunction		Application of the revised ARVC taskforce imaging criteria reduced overall prevalence of major and minor criteria; Specificity was preserved (94% 1994 criteria; 96% 2010 criteria) but may have reduced sensitivity
Tandri et al.(90)	Observational	30	LGE		12 (40%) met Task Force criteria for ARVD/C; 8 (67%) demonstrated +LGE in RV compared with 18 patients without ARVC ($p<0.001$)
Prati et al.(91)	Observational	32	LVEF/RVEF; Feature-tracking		Strain analysis by feature-tracking CMR provides additional value to assess global and regional RV dysfunction and dyssynchrony over conventional cine CMR imaging..
Inflammatory CM					
Kazmirczak et al.(92)	Observational	290	LVEF, LGE	Significant ventricular arrhythmia or sudden cardiac death	In known or suspected cardiac sarcoidosis, CMR helps identify all patients at risk for events. LGE of >5.7% identifies patients with LVEF >35% who would benefit from ICDs.
Velangi et al. (93)	Observational	290	LVEF, LGE	Significant ventricular arrhythmia or sudden cardiac death	RV systolic dysfunction alone in sarcoidosis was independently associated with all-cause mortality; RV LGE alone was independently associated with sudden cardiac death or significant ventricular arrhythmia
Smedema et al.(94)	Observational	58	LGE		Sensitivity of CMR to detect cardiac sarcoidosis was 100% (95% CI 78-100%) and specificity 78% (95% CI 64-89%); Overall accuracy of 83%
Smedema et al.(95)	Observational	55	LGE		CMR-based (LGE) detection of cardiac sarcoidosis was associated with overall duration of disease, function, and ventricular arrhythmias and may reveal early evidence of infiltration not detectable by standard assessment
Patel et al.(96)	Observational	81	LGE	Adverse events; cardiac death	26% of biopsy proven extracardiac sarcoid had cardiac involvement by LGE which translated to a 9 fold higher rate of adverse events and 11.5 fold higher rate of cardiac death than LGE negative patients.
Murtagh et al.(97)	Observational	205	LGE	Death/VT	20% patients with extracardiac sarcoid had +LGE
					10/12 (83%) experiencing death/VT were LGE+
					LGE burden best predictor of death/VT (AUC, 0.8); For every 1% increase in LGE burden, hazard of death/VT increased by 8%
Coleman et al.(98)	Metanalysis	760	LGE	All-cause mortality; Composite outcome: Ventricular arrhythmogenic events + all-cause mortality	In known or suspected cardiac sarcoid: LGE+ had higher odds for all-cause mortality (OR:3.06;$p<0.03$) and higher odds of composite outcome (OR:10.74; $p<0.00001$) – Annualized event rate 11.9% vs. 1.1%; $p<0.0001$)
Crouser et al.(99)	Observational	50	T2 mapping		Myocardial T2 is quantitatively abnormal in patients with sarcoidosis and may precede LGE; T2 elevation combined with LGE better predicts ECG abnormalities and arrhythmia.
SLE					

O'Neill et al.(100)	Observational	22	LGE	LGE vs. TTE	CMR detected more abnormalities using LGE (5/11) and 1/11 in control group than was detected by TTE (2/6 LGE+ cases)
Varma et al.(101)	Observational	75	Coronary Contrast-enhancement		Diffuse pattern for SLE and patchy/regional pattern for CAD detected by coronary contrast-enhancement
Mavrogeni et al.(102)	Observational	32	LV function; T2 STIR; LGE		Of 32 SLE patients with newly diagnosed HF: 16% had T2 ratio >2 c/w myocarditis; 16% had LV dysfunction; 34% MI, 28% diffuse subendocardial LGE; 15% LV dysfunction; LGE correlated with disease activity/duration and serum markers of SLE
Seneviratne et al.(103)	Observational	41	LGE		LGE>15% exhibited a reduced E/A ratio of 0.9±0.4 relative to the <15% and absent LGE subgroups
Abdel-Aty et al. (104)	Observational	20	T2-weighted SSFP; LVEF, early and late T1-weighted imaging		T2 ratio (myocardial/skeletal muscle) significantly higher in SLE (2.1±0.2) than inactive (1.8±0.2) or control groups (1.7±0.3)
Hinojar et al.(105)	Observational	76	LV mass, longitudinal strain, native T1 and T2		SLE+ patients had higher inflammatory markers, LV mass, native T1 and T2 and decreased longitudinal strain ($p<0.01$); T1 and T2 values on follow-up CMR exams were significantly reduced with intensified anti-inflammatory treatment ($p<0.001$)
Puntmann et al.(106)	Observational	33	Myocardial perfusion; pre- and post-contrast T1; strain; function; LGE		SLE patients had significantly decreased longitudinal strain; significantly increased native T1, ECV and + LGE (intramyocardial and pericardial)
Anderson-Fabry Disease					
Moon et al.(107)	Observational	26	LGE		50% of AFD patients had hyperenhancement ranging from 3.4-20.6% of total LV mass.
Sado et al.(108)	Observational	280	T1 mapping		Septal T1 was significantly lower and discriminated completely between AFD and other diseases without overlap
Thompson et al.(109)	Observational	31	T1 mapping; ECV		AFD patients had significantly lower myocardial T1 values compared to controls or patients with concentric hypertrophy despite similar ECV across all groups
Pica et al.(110)	Observational	63	T1 mapping		Native T1 mapping is reproducible in AFD patients ; Low native T1 is associated with abnormal echocardiographic strain measures prior to LVH onset
Hughes et al.(111)	RCT	15	LV mass; myocardial Gb_3		Significant reduction of CMR measured LV mass was detected 6 months after enzyme replacement therapy with agalsidase alfa compared to placebo ($p=0.041$).
Heart Failure					
Kanagala et al. (112)	Observational	140	LGE, T1 mapping for ECV		iECV (HR 1.7, $p=0.009$) was an independent predictor of outcome and associated with LV/LA remodeling and renal dysfunction, RV EDVi, LV mass/volume, max LA vol indexed in HFpEF compared to control
Duca et al. (113)	Observational	117		Combined endpoint: Hospitalization for heart failure and cardiac death	MOLLI-ECV ≥ 28.9% had decreased unadjusted event-free survival ($p=0.028$) but not after adjustment with clinical and invasive measurements.

Halliday et al.(114)	RCT	51	LVEF	Reduction in LVEF >10% and to less than 50%; LVEDV increase greater than 10% and to higher than normal range	Initial 6 months: 44% in treatment withdrawal arm relapsed (primary outcome) compared to none in the continued treatment arm. (Kaplan-Meier estimated event rate 45.7%, p=0.0001)
					Additional 6 month follow-up: 26 patients in treatment arm withdrew treatment with 9/26 experiencing relapse (Kaplan-Meier estimated event rate 36%).
Cancer					
Muehlberg et al.(115)	Observational	30	T1 and T2 mapping, ECV, LGE, LVEF	Anthracycline-induced cardiomyopathy (aCMP)= Drop of LVEF >10%	48 hours after first dose of anthracyclines, aCMP + patients had significantly lower myocardial T1 times compared to before therapy (1002 vs 957 ms, p<0.01) and decreased LV mass on therapy completion
Mahmood et al.(116)	Observational	35	LGE	MACE	Prevalence of myocarditis 1.14% within a median time of 34 days; lower steroid doses were associated with higher MACE
Fallah-Rad et al.(117)	Observational	42	LVEF		LVEDV and LVESV increased at 12-month follow-up; Decrease in LVEF from 66 to 47% by CMR; LGE detected early may indicate trastuzumab-related cardiotoxicity
Drafts et al.(118)	Observational	53	LVEF	Decline in EF	5% decline in LVEF by CMR; LV strain deteriorated (-17.7 to -15.1, p=0.0003)
Chaosuwannakit et al .(119)	Observational	40	LVEF	Decline in EF	5% decline in LVEF by CMR; Decreased aortic distensibility post anthracycline therapy
Jolly et al.(120)	Observational	72	CMR-Feature tracking	3-month serial change in global LV circumferential strain (GLCS)	GLCS worsened in patients at 3 months (-17.6 vs. 19%, p<0.0001) after administration of potentially cardiotoxic chemotherapy.
Grover et al. (121)	Observational	29	Aortic PWV, distensibility		Acute changes (increase in PWV and reduced distensibility in the asc. aorta) were noted and partially reverse a year after chemotherapy
Jordan et al. (122)	Observational	327	LV volumes; contrast-enhanced T1 and T2 weighted signal intensity before/after cardiotoxic therapy		CMR measures of T1 (14.1 to 15.9, p<0.05) occur with small but significant decline in LVEF (57 to 54%, p<0.001) 3 months post cardiotoxic medication administration.
Neilan et al. (123)	Observational	42	T1 and ECV		ECV elevated (0.36 vs 0.28, p<0.001) post-anthracycline treatmement compared to age- and gender-matched controls. Positive association between ECV and LV volume (r=0.65, p<0.0010; negative association between ECV and diastolic dysfunction (E'lat r=--.64, p<0.001)
Barthur et al. (124)	Observational	41	RV volumes; RVEF		Small but significant increase in RVEDV (p=0.002) and RVESV (p<0.001) at 6 months but not at 18 months post trastuzumab therapy.
Heart Transplantation					
Dolan et al.(125)	Observational	58	T2 and ECV	Acute cardiac allograft rejection	Combined model of age at CMR, global T2, ECV predictive of cardiac allograft rejection (AUC 0.84)
Hughes et al. (126)	Observational	152	LVEF, LGE	Death or MACE	Presence and the extent of LGE post-transplant are independently associated with the long-term risk of death or MACE. (HR

					2.88, p<0.001). Each 1% increase in LGE was independently associated with 6% increase in adjusted hazard for all-cause mortality or MACE (1.06, p<0.001).
Kazmirczak et al. (127)	Observational	57	Vasodilator stress CMR	MACE	Vasodilator stress CMR is safe in transplant recipients and predicts MACE.
Shenoy et al. (128)	Observational	152	LVEF, LGE	Death or MACE	CMR-FT GLS was independently associated with the long-term risk of death or MACE (adjusted HR was 1.15, p<0.001 for each 1% decline in GLS)
Marie et al. (129)	Observational	123	Myocardial T2 (black-blood)	Acute cardiac allograft rejection	Myocardial T2 (black-blood MRI) (>56ms) allowed accurate detection of moderate acute rejection evidenced at baseline biopsy (sensitivity 89%, specificity 70%, p<0.0001)
Bonnemains et al. (130)	Observational	196	Myocardial T2	Acute cardiac allograft rejection	T2 values above 60ms were associated with relative risk of rejection higher than 2.0 and strongly associated with presence of rejection on biopsy (p<0.0001)
Coehlo-Filho et al. (131)	Observational	26	T1 mapping, LVEF, LV mass, LGE, ECV, intracellular lifetime of water		OHT recipients had normal LVEF with higher LV mass compared to controls; ECV and intracellular lifetime of water was higher post-OHT (0.39 vs 0.28, p<0.001; τ_{ic} 0.12 vs. 0.08, p<0.001)
Usman et al. (132)	Observational	53	Quantitative T2 mapping		Grade 0R 52.5 ± 2.2ms Grade 1R 53.1 ± 3.3ms Grade 2R 59.2 ± 3.3ms Hemodynamic rejection 61.1±1.8ms (p<0.05) without evidence of ventricular dysfunction
Feingold et al. (133)	Observational	25	ECV, Fibrosis by picrosirius red staining CVF		ECV was moderately correlated with CVF (r=0.47, p=0.019), no difference compared to normal controls (ECV 25.1±3.0 vs 23.7 ±2.0%, p=0.09)
Imran et al.(134)	Observational	112	Native T1		Native T1 cutoff value of 1029ms had sensitivity (93%), specificity (79%), and NPV (99%) for detection of cardiac allograft rejection.
Taylor et al. (135)	Observational	50	LVEF, T2 weighted edema imaging, EGE, LGE		Patients with EMB confirmed rejection had elevated early relative myocardial contrast enhancement (4.1 vs. 2.8, p<0.001); CMR edema had sensitivity 100% and specificity of 73% compared with EMB.

1. Arai AE, Schulz-Menger J, Berman D et al. Gadobutrol-Enhanced Cardiac Magnetic Resonance Imaging for Detection of Coronary Artery Disease. Journal of the American College of Cardiology 2020;76:1536-1547.
2. Heitner JF, Kim RJ, Kim HW et al. Prognostic Value of Vasodilator Stress Cardiac Magnetic Resonance Imaging: A Multicenter Study With 48 000 Patient-Years of Follow-up. JAMA Cardiol 2019;4:256-264.
3. Kwong RY, Ge Y, Steel K et al. Cardiac Magnetic Resonance Stress Perfusion Imaging for Evaluation of Patients With Chest Pain. Journal of the American College of Cardiology 2019;74:1741-1755.
4. Pontone G, Andreini D, Guaricci AI et al. The STRATEGY Study (Stress Cardiac Magnetic Resonance Versus Computed Tomography Coronary Angiography for

the Management of Symptomatic Revascularized Patients). Circulation: Cardiovascular Imaging 2016;9:e005171.
5. Schwitter J, Wacker CM, Wilke N et al. MR-IMPACT II: Magnetic Resonance Imaging for Myocardial Perfusion Assessment in Coronary artery disease Trial: perfusion-cardiac magnetic resonance vs. single-photon emission computed tomography for the detection of coronary artery disease: a comparative multicentre, multivendor trial. European Heart Journal 2012;34:775-781.
6. Bruder O, Wagner A, Lombardi M et al. European cardiovascular magnetic resonance (EuroCMR) registry – multi national results from 57 centers in 15 countries. Journal of Cardiovascular Magnetic Resonance 2013;15:9.
7. Nagel E, Greenwood JP, McCann GP et al. Magnetic Resonance Perfusion or Fractional Flow Reserve in Coronary Disease. New England Journal of Medicine 2019;380:2418-2428.
8. Greenwood JP, Maredia N, Younger JF et al. Cardiovascular magnetic resonance and single-photon emission computed tomography for diagnosis of coronary heart disease (CE-MARC): a prospective trial. Lancet 2012;379:453-60.
9. Greenwood JP, Ripley DP, Berry C et al. Effect of Care Guided by Cardiovascular Magnetic Resonance, Myocardial Perfusion Scintigraphy, or NICE Guidelines on Subsequent Unnecessary Angiography Rates: The CE-MARC 2 Randomized Clinical Trial. Jama 2016;316:1051-60.
10. Greenwood JP, Herzog BA, Brown JM et al. Prognostic Value of Cardiovascular Magnetic Resonance and Single-Photon Emission Computed Tomography in Suspected Coronary Heart Disease: Long-Term Follow-up of a Prospective, Diagnostic Accuracy Cohort Study. Ann Intern Med 2016;165:1-9.
11. Walker S, Girardin F, McKenna C et al. Cost-effectiveness of cardiovascular magnetic resonance in the diagnosis of coronary heart disease: an economic evaluation using data from the CE-MARC study. Heart 2013;99:873-881.
12. Eitel I, Stiermaier T, Lange T et al. Cardiac Magnetic Resonance Myocardial Feature Tracking for Optimized Prediction of Cardiovascular Events Following Myocardial Infarction. JACC: Cardiovascular Imaging 2018;11:1433-1444.
13. Rijlaarsdam-Hermsen D, Lo-Kioeng-Shioe M, van Domburg RT, Deckers JW, Kuijpers D, van Dijkman PRM. Stress-Only Adenosine CMR Improves Diagnostic Yield in Stable Symptomatic Patients With Coronary Artery Calcium. JACC: Cardiovascular Imaging 2020;13:1152-1160.
14. McCann GP, Khan JN, Greenwood JP et al. Complete Versus Lesion-Only Primary PCI. Journal of the American College of Cardiology 2015;66:2713-2724.
15. Pontone G, Guaricci AI, Andreini D et al. Prognostic Stratification of Patients With ST-Segment-Elevation Myocardial Infarction (PROSPECT): A Cardiac Magnetic Resonance Study. Circ Cardiovasc Imaging 2017;10.
16. Heydari B, Abdullah S, Pottala JV et al. Effect of Omega-3 Acid Ethyl Esters on Left Ventricular Remodeling After Acute Myocardial Infarction. Circulation 2016;134:378-391.
17. McCartney PJ, Eteiba H, Maznyczka AM et al. Effect of Low-Dose Intracoronary Alteplase During Primary Percutaneous Coronary Intervention on Microvascular Obstruction in Patients With Acute Myocardial Infarction: A Randomized Clinical Trial. Jama 2019;321:56-68.

18. Nazir SA, McCann GP, Greenwood JP et al. Strategies to attenuate micro-vascular obstruction during P-PCI: the randomized reperfusion facilitated by local adjunctive therapy in ST-elevation myocardial infarction trial. Eur Heart J 2016;37:1910-9.
19. Piccolo R, Eitel I, Galasso G et al. 1-Year Outcomes With Intracoronary Abciximab in Diabetic Patients Undergoing Primary Percutaneous Coronary Intervention. Journal of the American College of Cardiology 2016;68:727-738.
20. Thomson LE, Wei J, Agarwal M et al. Cardiac magnetic resonance myocardial perfusion reserve index is reduced in women with coronary microvascular dysfunction. A National Heart, Lung, and Blood Institute-sponsored study from the Women's Ischemia Syndrome Evaluation. Circ Cardiovasc Imaging 2015;8.
21. Williams RP, de Waard GA, De Silva K et al. Doppler Versus Thermodilution-Derived Coronary Microvascular Resistance to Predict Coronary Microvascular Dysfunction in Patients With Acute Myocardial Infarction or Stable Angina Pectoris. Am J Cardiol 2018;121:1-8.
22. Zorach B, Shaw P, Bourque J et al. Quantitative cardiovascular magnetic resonance perfusion imaging identifies reduced flow reserve in microvascular coronary artery disease. Journal of Cardiovascular Magnetic Resonance 2018;20.
23. Kotecha T, Martinez-Naharro A, Boldrini M et al. Automated Pixel-Wise Quantitative Myocardial Perfusion Mapping by CMR to Detect Obstructive Coronary Artery Disease and Coronary Microvascular Dysfunction: Validation Against Invasive Coronary Physiology. JACC Cardiovasc Imaging 2019;12:1958-1969.
24. Lurz P, Luecke C, Eitel I et al. Comprehensive Cardiac Magnetic Resonance Imaging in Patients With Suspected Myocarditis: The MyoRacer-Trial. J Am Coll Cardiol 2016;67:1800-1811.
25. Leong DP, Chakrabarty A, Shipp N et al. Effects of myocardial fibrosis and ventricular dyssynchrony on response to therapy in new-presentation idiopathic dilated cardiomyopathy: insights from cardiovascular magnetic resonance and echocardiography. European Heart Journal 2011;33:640-648.
26. Gulati A, Jabbour A, Ismail TF et al. Association of fibrosis with mortality and sudden cardiac death in patients with nonischemic dilated cardiomyopathy. Jama 2013;309:896-908.
27. Puntmann VO, Carr-White G, Jabbour A et al. T1-Mapping and Outcome in Nonischemic Cardiomyopathy: All-Cause Mortality and Heart Failure. JACC Cardiovasc Imaging 2016;9:40-50.
28. Weng Z, Yao J, Chan RH et al. Prognostic Value of LGE-CMR in HCM: A Meta-Analysis. JACC Cardiovasc Imaging 2016;9:1392-1402.
29. Neubauer S, Kolm P, Ho CY et al. Distinct Subgroups in Hypertrophic Cardiomyopathy in the NHLBI HCM Registry. Journal of the American College of Cardiology 2019;74:2333-2345.
30. Chan RH, Maron BJ, Olivotto I et al. Prognostic value of quantitative contrast-enhanced cardiovascular magnetic resonance for the evaluation of sudden death risk in patients with hypertrophic cardiomyopathy. Circulation 2014;130:484-95.

31. Dass S, Suttie JJ, Piechnik SK et al. Myocardial Tissue Characterization Using Magnetic Resonance Noncontrast T1 Mapping in Hypertrophic and Dilated Cardiomyopathy. Circulation: Cardiovascular Imaging 2012;5:726-733.
32. Hinojar R, Varma N, Child N et al. T1 Mapping in Discrimination of Hypertrophic Phenotypes: Hypertensive Heart Disease and Hypertrophic Cardiomyopathy: Findings From the International T1 Multicenter Cardiovascular Magnetic Resonance Study. Circ Cardiovasc Imaging 2015;8.
33. Puntmann VO, Voigt T, Chen Z et al. Native T1 mapping in differentiation of normal myocardium from diffuse disease in hypertrophic and dilated cardiomyopathy. JACC Cardiovasc Imaging 2013;6:475-84.
34. Ho CY, Abbasi SA, Neilan TG et al. T1 measurements identify extracellular volume expansion in hypertrophic cardiomyopathy sarcomere mutation carriers with and without left ventricular hypertrophy. Circ Cardiovasc Imaging 2013;6:415-22.
35. Mc LA, Ellims AH, Prabhu S et al. Diffuse Ventricular Fibrosis on Cardiac Magnetic Resonance Imaging Associates With Ventricular Tachycardia in Patients With Hypertrophic Cardiomyopathy. J Cardiovasc Electrophysiol 2016;27:571-80.
36. Kawel N, Nacif M, Arai AE et al. Trabeculated (noncompacted) and compact myocardium in adults: the multi-ethnic study of atherosclerosis. Circ Cardiovasc Imaging 2012;5:357-66.
37. Weir-McCall JR, Yeap PM, Papagiorcopulo C et al. Left Ventricular Noncompaction: Anatomical Phenotype or Distinct Cardiomyopathy? J Am Coll Cardiol 2016;68:2157-2165.
38. Jacquier A, Thuny F, Jop B et al. Measurement of trabeculated left ventricular mass using cardiac magnetic resonance imaging in the diagnosis of left ventricular non-compaction. Eur Heart J 2010;31:1098-104.
39. Andreini D, Pontone G, Bogaert J et al. Long-Term Prognostic Value of Cardiac Magnetic Resonance in Left Ventricle Noncompaction: A Prospective Multicenter Study. J Am Coll Cardiol 2016;68:2166-2181.
40. Hor KN, Wansapura J, Markham LW et al. Circumferential strain analysis identifies strata of cardiomyopathy in Duchenne muscular dystrophy: a cardiac magnetic resonance tagging study. J Am Coll Cardiol 2009;53:1204-10.
41. Becker S, Florian A, Patrascu A et al. Identification of cardiomyopathy associated circulating miRNA biomarkers in patients with muscular dystrophy using a complementary cardiovascular magnetic resonance and plasma profiling approach. Journal of Cardiovascular Magnetic Resonance 2016;18:25.
42. Hor KN, Taylor MD, Al-Khalidi HR et al. Prevalence and distribution of late gadolinium enhancement in a large population of patients with Duchenne muscular dystrophy: effect of age and left ventricular systolic function. J Cardiovasc Magn Reson 2013;15:107.
43. Tandon A, Villa CR, Hor KN et al. Myocardial Fibrosis Burden Predicts Left Ventricular Ejection Fraction and Is Associated With Age and Steroid Treatment Duration in Duchenne Muscular Dystrophy. Journal of the American Heart Association 2015;4:e001338.
44. Taylor M, Jefferies J, Byrne B et al. Cardiac and skeletal muscle effects in the randomized HOPE-Duchenne trial. Neurology 2019;92:e866-e878.

45. Martinez-Naharro A, Kotecha T, Norrington K et al. Native T1 and Extracellular Volume in Transthyretin Amyloidosis. JACC Cardiovasc Imaging 2019;12:810-819.
46. Martinez-Naharro A, Abdel-Gadir A, Treibel T et al. CMR-Verified Regression of Cardiac AL Amyloid After Chemotherapy. JACC: Cardiovascular Imaging 2017;11.
47. Fontana M, Banypersad SM, Treibel TA et al. Differential Myocyte Responses in Patients with Cardiac Transthyretin Amyloidosis and Light-Chain Amyloidosis: A Cardiac MR Imaging Study. Radiology 2015;277:388-97.
48. Kotecha T, Martinez-Naharro A, Treibel TA et al. Myocardial Edema and Prognosis in Amyloidosis. J Am Coll Cardiol 2018;71:2919-2931.
49. Banypersad SM, Fontana M, Maestrini V et al. T1 mapping and survival in systemic light-chain amyloidosis. Eur Heart J 2015;36:244-51.
50. Fontana M, Banypersad SM, Treibel TA et al. Native T1 mapping in transthyretin amyloidosis. JACC Cardiovasc Imaging 2014;7:157-65.
51. Karamitsos TD, Piechnik SK, Banypersad SM et al. Noncontrast T1 mapping for the diagnosis of cardiac amyloidosis. JACC Cardiovasc Imaging 2013;6:488-97.
52. Banypersad SM, Sado DM, Flett AS et al. Quantification of myocardial extracellular volume fraction in systemic AL amyloidosis: an equilibrium contrast cardiovascular magnetic resonance study. Circ Cardiovasc Imaging 2013;6:34-9.
53. Fontana M, Pica S, Reant P et al. Prognostic Value of Late Gadolinium Enhancement Cardiovascular Magnetic Resonance in Cardiac Amyloidosis. Circulation 2015;132:1570-9.
54. White JA, Kim HW, Shah D et al. CMR imaging with rapid visual T1 assessment predicts mortality in patients suspected of cardiac amyloidosis. JACC Cardiovasc Imaging 2014;7:143-56.
55. Kirk P, Roughton M, Porter JB et al. Cardiac T2* magnetic resonance for prediction of cardiac complications in thalassemia major. Circulation 2009;120:1961-8.
56. Leonardi B, Margossian R, Colan SD, Powell AJ. Relationship of magnetic resonance imaging estimation of myocardial iron to left ventricular systolic and diastolic function in thalassemia. JACC Cardiovasc Imaging 2008;1:572-8.
57. Modell B, Khan M, Darlison M, Westwood MA, Ingram D, Pennell DJ. Improved survival of thalassaemia major in the UK and relation to T2* cardiovascular magnetic resonance. Journal of Cardiovascular Magnetic Resonance 2008;10:42.
58. Anderson LJ, Holden S, Davis B et al. Cardiovascular T2-star (T2*) magnetic resonance for the early diagnosis of myocardial iron overload. Eur Heart J 2001;22:2171-9.
59. Anderson LJ, Westwood MA, Holden S et al. Myocardial iron clearance during reversal of siderotic cardiomyopathy with intravenous desferrioxamine: a prospective study using T2* cardiovascular magnetic resonance. British Journal of Haematology 2004;127:348-355.
60. Anderson LJ, Wonke B, Prescott E, Holden S, Malcolm Walker J, Pennell DJ. Comparison of effects of oral deferiprone and subcutaneous desferrioxamine

on myocardial iron concentrations and ventricular function in beta-thalassaemia. The Lancet 2002;360:516-520.
61. Tanner MA, Galanello R, Dessi C et al. A randomized, placebo-controlled, double-blind trial of the effect of combined therapy with deferoxamine and deferiprone on myocardial iron in thalassemia major using cardiovascular magnetic resonance. Circulation 2007;115:1876-84.
62. Singh A, Greenwood JP, Berry C et al. Comparison of exercise testing and CMR measured myocardial perfusion reserve for predicting outcome in asymptomatic aortic stenosis: the PRognostic Importance of MIcrovascular Dysfunction in Aortic Stenosis (PRIMID AS) Study. European heart journal 2017;38:1222-1229.
63. Cavalcante JL, Kusunose K, Obuchowski NA et al. Prognostic Impact of Ischemic Mitral Regurgitation Severity and Myocardial Infarct Quantification by Cardiovascular Magnetic Resonance. JACC: Cardiovascular Imaging 2020;13:1489-1501.
64. Uretsky S, Gillam L, Lang R et al. Discordance between echocardiography and MRI in the assessment of mitral regurgitation severity: a prospective multicenter trial. J Am Coll Cardiol 2015;65:1078-88.
65. Everett RJ, Treibel TA, Fukui M et al. Extracellular Myocardial Volume in Patients With Aortic Stenosis. J Am Coll Cardiol 2020;75:304-316.
66. Loudon BL, Ntatsaki E, Newsome S et al. Osteoprotegerin and Myocardial Fibrosis in Patients with Aortic Stenosis. Scientific Reports 2018;8:14550.
67. Ahn JH, Kim SM, Park SJ et al. Coronary Microvascular Dysfunction as a Mechanism of Angina in Severe AS: Prospective Adenosine-Stress CMR Study. J Am Coll Cardiol 2016;67:1412-1422.
68. Biederman RW, Magovern JA, Grant SB et al. LV reverse remodeling imparted by aortic valve replacement for severe aortic stenosis; is it durable? A cardiovascular MRI study sponsored by the American Heart Association. J Cardiothorac Surg 2011;6:53.
69. Hart SA, Devendra GP, Kim YY et al. PINOT NOIR: pulmonic insufficiency improvement with nitric oxide inhalational response. J Cardiovasc Magn Reson 2013;15:75.
70. Dweck MR, Joshi S, Murigu T et al. Left ventricular remodeling and hypertrophy in patients with aortic stenosis: insights from cardiovascular magnetic resonance. J Cardiovasc Magn Reson 2012;14:50.
71. Barone-Rochette G, Piérard S, De Meester de Ravenstein C et al. Prognostic Significance of LGE by CMR in Aortic Stenosis Patients Undergoing Valve Replacement. Journal of the American College of Cardiology 2014;64:144-154.
72. Rajesh GN, Thottian JJ, Subramaniam G, Desabandhu V, Sajeev CG, Krishnan MN. Prevalence and prognostic significance of left ventricular myocardial late gadolinium enhancement in severe aortic stenosis. Indian Heart Journal 2017;69:742-750.
73. Musa TA, Treibel TA, Vassiliou VS et al. Myocardial Scar and Mortality in Severe Aortic Stenosis. Circulation 2018;138:1935-1947.
74. Chin CWL, Everett RJ, Kwiecinski J et al. Myocardial Fibrosis and Cardiac Decompensation in Aortic Stenosis. JACC: Cardiovascular Imaging 2017;10:1320-1333.

75. Lee H, Park J-B, Yoon YE et al. Noncontrast Myocardial T1 Mapping by Cardiac Magnetic Resonance Predicts Outcome in Patients With Aortic Stenosis. JACC: Cardiovascular Imaging 2018;11:974-983.
76. Kang DH, Park SW, Song JK et al. Long-term clinical and echocardiographic outcome of percutaneous mitral valvuloplasty: randomized comparison of Inoue and double-balloon techniques. J Am Coll Cardiol 2000;35:169-75.
77. Treibel TA, Kozor R, Schofield R et al. Reverse Myocardial Remodeling Following Valve Replacement in Patients With Aortic Stenosis. Journal of the American College of Cardiology 2018;71:860-871.
78. Myerson SG, d'Arcy J, Mohiaddin R et al. Aortic Regurgitation Quantification Using Cardiovascular Magnetic Resonance. Circulation 2012;126:1452-1460.
79. Myerson SG, d'Arcy J, Christiansen JP et al. Determination of Clinical Outcome in Mitral Regurgitation With Cardiovascular Magnetic Resonance Quantification. Circulation 2016;133:2287-96.
80. Chaikriangkrai K, Lopez-Mattei JC, Lawrie G et al. Prognostic Value of Delayed Enhancement Cardiac Magnetic Resonance Imaging in Mitral Valve Repair. The Annals of Thoracic Surgery 2014;98:1557-1563.
81. Azevedo CF, Nigri M, Higuchi ML et al. Prognostic Significance of Myocardial Fibrosis Quantification by Histopathology and Magnetic Resonance Imaging in Patients With Severe Aortic Valve Disease. Journal of the American College of Cardiology 2010;56:278-287.
82. Prabhu S, Taylor AJ, Costello BT et al. Catheter Ablation Versus Medical Rate Control in Atrial Fibrillation and Systolic Dysfunction: The CAMERA-MRI Study. Journal of the American College of Cardiology 2017;70:1949-1961.
83. Paetsch I, Sommer P, Jahnke C et al. Clinical workflow and applicability of electrophysiological cardiovascular magnetic resonance-guided radiofrequency ablation of isthmus-dependent atrial flutter. European Heart Journal - Cardiovascular Imaging 2018;20:147-156.
84. Bilchick KC, Auger DA, Abdishektaei M et al. CMR DENSE and the Seattle Heart Failure Model Inform Survival and Arrhythmia Risk After CRT. JACC Cardiovasc Imaging 2020;13:924-936.
85. Klem I, Weinsaft JW, Bahnson TD et al. Assessment of myocardial scarring improves risk stratification in patients evaluated for cardiac defibrillator implantation. J Am Coll Cardiol 2012;60:408-20.
86. Halliday BP, Gulati A, Ali A et al. Association Between Midwall Late Gadolinium Enhancement and Sudden Cardiac Death in Patients With Dilated Cardiomyopathy and Mild and Moderate Left Ventricular Systolic Dysfunction. Circulation 2017;135:2106-2115.
87. Leyva F, Foley PW, Chalil S et al. Cardiac resynchronization therapy guided by late gadolinium-enhancement cardiovascular magnetic resonance. J Cardiovasc Magn Reson 2011;13:29.
88. Leyva F, Taylor RJ, Foley PWX et al. Left Ventricular Midwall Fibrosis as a Predictor of Mortality and Morbidity After Cardiac Resynchronization Therapy in Patients With Nonischemic Cardiomyopathy. Journal of the American College of Cardiology 2012;60:1659-1667.
89. Vermes E, Strohm O, Otmani A, Childs H, Duff H, Friedrich MG. Impact of the Revision of Arrhythmogenic Right Ventricular Cardiomyopathy/Dysplasia Task

Force Criteria on Its Prevalence by CMR Criteria. JACC: Cardiovascular Imaging 2011;4:282-287.
90. Tandri H, Saranathan M, Rodriguez ER et al. Noninvasive detection of myocardial fibrosis in arrhythmogenic right ventricular cardiomyopathy using delayed-enhancement magnetic resonance imaging. J Am Coll Cardiol 2005;45:98-103.
91. Prati G, Vitrella G, Allocca G et al. Right Ventricular Strain and Dyssynchrony Assessment in Arrhythmogenic Right Ventricular Cardiomyopathy: Cardiac Magnetic Resonance Feature-Tracking Study. Circ Cardiovasc Imaging 2015;8:e003647; discussion e003647.
92. Kazmirczak F, Chen K-HA, Adabag S et al. Assessment of the 2017 AHA/ACC/HRS Guideline Recommendations for Implantable Cardioverter-Defibrillator Implantation in Cardiac Sarcoidosis. Circulation: Arrhythmia and Electrophysiology 2019;12:e007488.
93. Velangi PS, Chen KA, Kazmirczak F et al. Right Ventricular Abnormalities on Cardiovascular Magnetic Resonance Imaging in Patients With Sarcoidosis. JACC Cardiovasc Imaging 2020;13:1395-1405.
94. Smedema JP, Snoep G, van Kroonenburgh MP et al. Evaluation of the accuracy of gadolinium-enhanced cardiovascular magnetic resonance in the diagnosis of cardiac sarcoidosis. J Am Coll Cardiol 2005;45:1683-90.
95. Smedema JP, Snoep G, van Kroonenburgh MP et al. The additional value of gadolinium-enhanced MRI to standard assessment for cardiac involvement in patients with pulmonary sarcoidosis. Chest 2005;128:1629-37.
96. Patel MR, Cawley PJ, Heitner JF et al. Detection of Myocardial Damage in Patients With Sarcoidosis. Circulation 2009;120:1969-1977.
97. Murtagh G, Laffin LJ, Beshai JF et al. Prognosis of Myocardial Damage in Sarcoidosis Patients With Preserved Left Ventricular Ejection Fraction: Risk Stratification Using Cardiovascular Magnetic Resonance. Circ Cardiovasc Imaging 2016;9:e003738.
98. Coleman GC, Shaw PW, Balfour PC, Jr. et al. Prognostic Value of Myocardial Scarring on CMR in Patients With Cardiac Sarcoidosis. JACC Cardiovasc Imaging 2017;10:411-420.
99. Crouser ED, Ono C, Tran T, He X, Raman SV. Improved detection of cardiac sarcoidosis using magnetic resonance with myocardial T2 mapping. Am J Respir Crit Care Med 2014;189:109-12.
100. O'Neill SG, Woldman S, Bailliard F et al. Cardiac magnetic resonance imaging in patients with systemic lupus erythematosus. Ann Rheum Dis 2009;68:1478-81.
101. Varma N, Hinojar R, D'Cruz D et al. Coronary vessel wall contrast enhancement imaging as a potential direct marker of coronary involvement: integration of findings from CAD and SLE patients. JACC Cardiovasc Imaging 2014;7:762-70.
102. Mavrogeni S, Karabela G, Stavropoulos E et al. Heart failure imaging patterns in systemic lupus erythematosus. Evaluation using cardiovascular magnetic resonance. International Journal of Cardiology 2014;176:559-561.
103. Seneviratne MG, Grieve SM, Figtree GA et al. Prevalence, distribution and clinical correlates of myocardial fibrosis in systemic lupus erythematosus: a cardiac magnetic resonance study. Lupus 2016;25:573-81.

104. Abdel-Aty H, Siegle N, Natusch A et al. Myocardial tissue characterization in systemic lupus erythematosus: value of a comprehensive cardiovascular magnetic resonance approach. Lupus 2008;17:561-7.
105. Hinojar R, Foote L, Sangle S et al. Native T1 and T2 mapping by CMR in lupus myocarditis: Disease recognition and response to treatment. Int J Cardiol 2016;222:717-726.
106. Puntmann VO, D'Cruz D, Smith Z et al. Native myocardial T1 mapping by cardiovascular magnetic resonance imaging in subclinical cardiomyopathy in patients with systemic lupus erythematosus. Circ Cardiovasc Imaging 2013;6:295-301.
107. Moon JC, Sachdev B, Elkington AG et al. Gadolinium enhanced cardiovascular magnetic resonance in Anderson-Fabry disease. Evidence for a disease specific abnormality of the myocardial interstitium. Eur Heart J 2003;24:2151-5.
108. Sado D, White SK, Piechnik SK et al. Native T1 lowering in iron overload and Anderson Fabry disease; a novel and early marker of disease: J Cardiovasc Magn Reson. 2013 Jan 30;15(Suppl 1):O71. doi: 10.1186/1532-429X-15-S1-O71. eCollection 2013.
109. Thompson RB, Chow K, Khan A et al. T₁ Mapping With Cardiovascular MRI Is Highly Sensitive for Fabry Disease Independent of Hypertrophy and Sex. Circulation: Cardiovascular Imaging 2013;6:637-645.
110. Pica S, Sado DM, Maestrini V et al. Reproducibility of native myocardial T1 mapping in the assessment of Fabry disease and its role in early detection of cardiac involvement by cardiovascular magnetic resonance. Journal of Cardiovascular Magnetic Resonance 2014;16:99.
111. Hughes DA, Elliott PM, Shah J et al. Effects of enzyme replacement therapy on the cardiomyopathy of Anderson-Fabry disease: a randomised, double-blind, placebo-controlled clinical trial of agalsidase alfa. Heart 2008;94:153-8.
112. Kanagala P, Cheng ASH, Singh A et al. Relationship Between Focal and Diffuse Fibrosis Assessed by CMR and Clinical Outcomes in Heart Failure With Preserved Ejection Fraction. JACC Cardiovasc Imaging 2019;12:2291-2301.
113. Duca F, Kammerlander AA, Zotter-Tufaro C et al. Interstitial Fibrosis, Functional Status, and Outcomes in Heart Failure With Preserved Ejection Fraction. Circulation: Cardiovascular Imaging 2016;9:e005277.
114. Halliday BP, Wassall R, Lota AS et al. Withdrawal of pharmacological treatment for heart failure in patients with recovered dilated cardiomyopathy (TRED-HF): an open-label, pilot, randomised trial. Lancet 2019;393:61-73.
115. Muehlberg F, Funk S, Zange L et al. Native myocardial T1 time can predict development of subsequent anthracycline-induced cardiomyopathy. ESC Heart Fail 2018;5:620-629.
116. Mahmood SS, Fradley MG, Cohen JV et al. Myocarditis in Patients Treated With Immune Checkpoint Inhibitors. J Am Coll Cardiol 2018;71:1755-1764.
117. Fallah-Rad N, Walker JR, Wassef A et al. The Utility of Cardiac Biomarkers, Tissue Velocity and Strain Imaging, and Cardiac Magnetic Resonance Imaging in Predicting Early Left Ventricular Dysfunction in Patients With Human Epidermal Growth Factor Receptor II–Positive Breast Cancer Treated With Adjuvant Trastuzumab Therapy. Journal of the American College of Cardiology 2011;57:2263-2270.

118. Drafts BC, Twomley KM, D'Agostino R, Jr. et al. Low to moderate dose anthracycline-based chemotherapy is associated with early noninvasive imaging evidence of subclinical cardiovascular disease. JACC Cardiovasc Imaging 2013;6:877-85.
119. Chaosuwannakit N, D'Agostino R, Jr., Hamilton CA et al. Aortic stiffness increases upon receipt of anthracycline chemotherapy. J Clin Oncol 2010;28:166-72.
120. Jolly M-P, Jordan JH, Meléndez GC, McNeal GR, D'Agostino RB, Hundley WG. Automated assessments of circumferential strain from cine CMR correlate with LVEF declines in cancer patients early after receipt of cardio-toxic chemotherapy. Journal of Cardiovascular Magnetic Resonance 2017;19:59.
121. Grover S, Lou PW, Bradbrook C et al. Early and late changes in markers of aortic stiffness with breast cancer therapy. Intern Med J 2015;45:140-7.
122. Jordan JH, Vasu S, Morgan TM et al. Anthracycline-Associated T1 Mapping Characteristics Are Elevated Independent of the Presence of Cardiovascular Comorbidities in Cancer Survivors. Circ Cardiovasc Imaging 2016;9.
123. Neilan TG, Coelho-Filho OR, Shah RV et al. Myocardial extracellular volume by cardiac magnetic resonance imaging in patients treated with anthracycline-based chemotherapy. Am J Cardiol 2013;111:717-22.
124. Barthur A, Brezden-Masley C, Connelly KA et al. Longitudinal assessment of right ventricular structure and function by cardiovascular magnetic resonance in breast cancer patients treated with trastuzumab: a prospective observational study. Journal of Cardiovascular Magnetic Resonance 2017;19:44.
125. Dolan RS, Rahsepar AA, Blaisdell J et al. Multiparametric Cardiac Magnetic Resonance Imaging Can Detect Acute Cardiac Allograft Rejection After Heart Transplantation. JACC Cardiovasc Imaging 2019;12:1632-1641.
126. Hughes A, Okasha O, Farzaneh-Far A et al. Myocardial Fibrosis and Prognosis in Heart Transplant Recipients. Circulation: Cardiovascular Imaging 2019;12:e009060.
127. Kazmirczak F, Nijjar PS, Zhang L et al. Safety and prognostic value of regadenoson stress cardiovascular magnetic resonance imaging in heart transplant recipients. Journal of Cardiovascular Magnetic Resonance 2019;21:9.
128. Shenoy C, Romano S, Hughes A et al. Cardiac Magnetic Resonance Feature Tracking Global Longitudinal Strain and Prognosis After Heart Transplantation. JACC: Cardiovascular Imaging 2020;13:1934-1942.
129. Marie PY, Angioï M, Carteaux JP et al. Detection and prediction of acute heart transplant rejection with the myocardial T2 determination provided by a black-blood magnetic resonance imaging sequence. J Am Coll Cardiol 2001;37:825-31.
130. Bonnemains L, Villemin T, Escanye JM et al. Diagnostic and prognostic value of MRI T2 quantification in heart transplant patients. Transpl Int 2014;27:69-76.
131. Coelho-Filho O, Shah R, Lavagnoli C et al. Myocardial tissue remodeling after orthotopic heart transplantation: a pilot cardiac magnetic resonance study. The International Journal of Cardiovascular Imaging 2016;34.
132. Usman AA, Taimen K, Wasielewski M et al. Cardiac magnetic resonance T2 mapping in the monitoring and follow-up of acute cardiac transplant rejection: a pilot study. Circ Cardiovasc Imaging 2012;5:782-90.

133. Feingold B, Salgado CM, Reyes-Múgica M et al. Diffuse myocardial fibrosis among healthy pediatric heart transplant recipients: Correlation of histology, cardiovascular magnetic resonance, and clinical phenotype. Pediatr Transplant 2017;21.
134. Imran M, Wang L, McCrohon J et al. Native T(1) Mapping in the Diagnosis of Cardiac Allograft Rejection: A Prospective Histologically Validated Study. JACC Cardiovasc Imaging 2019;12:1618-1628.
135. Taylor AJ, Vaddadi G, Pfluger H et al. Diagnostic performance of multisequential cardiac magnetic resonance imaging in acute cardiac allograft rejection. Eur J Heart Fail 2010;12:45-51.